Net ecosystem carbon exchange and the greenhouse gas balance of tidal marshes along an estuarine salinity gradient

**Nathaniel B. Weston · Scott C. Neubauer ·
David J. Velinsky · Melanie A. Vile**

Abstract Tidal wetlands are productive ecosystems with the capacity to sequester large amounts of carbon (C), but we know relatively little about the impact of climate change on wetland C cycling in lower salinity (oligohaline and tidal freshwater) coastal marshes. In this study we assessed plant production, C cycling and sequestration, and microbial organic matter mineralization at tidal freshwater, oligohaline, and salt marsh sites along the salinity gradient in the Delaware River Estuary over four years. We measured aboveground plant biomass, carbon dioxide (CO_2) and methane (CH_4) exchange between the marsh and atmosphere, microbial sulfate reduction and methanogenesis in marsh soils, soil biogeochemistry, and C sequestration with radiodating of soils. A simple model was constructed to estimate monthly and annually integrated rates of gross ecosystem production (GEP), ecosystem respiration (ER) to carbon dioxide (ER_{CO_2}) or methane (ER_{CH_4}), net ecosystem production (NEP), the contribution of sulfate reduction and methanogenesis to ER, and the greenhouse gas (GHG) source or sink status of the wetland for 2 years (2007 and 2008). All three marsh types were highly productive but evidenced different patterns of C sequestration and GHG source/sink status. The contribution of sulfate reduction to total ER increased along the salinity gradient from tidal freshwater to salt marsh. The *Spartina alterniflora* dominated salt marsh was a C sink as indicated by both NEP (~ 140 g C m^{-2} year^{-1}) and ^{210}Pb radiodating (336 g C m^{-2} year^{-1}), a minor sink for atmospheric CH_4, and a GHG sink (~ 620 g $CO_{2\text{-eq}}$ m^{-2} year^{-1}). The tidal freshwater marsh was a source of CH_4 to the atmosphere (~ 22 g C–CH$_4$ m^{-2} year^{-1}). There were large interannual differences in plant production and therefore C and GHG source/sink status at the tidal freshwater marsh, though ^{210}Pb radiodating indicated modest C accretion (110 g C m^{-2} year^{-1}). The oligohaline marsh site experienced seasonal saltwater intrusion in the late summer and fall (up to 10 mS cm^{-1}) and the *Zizania aquatica* monoculture at this site responded with sharp declines in biomass and GEP in late summer. Salinity intrusion was also linked to large effluxes of CH_4 at the

N. B. Weston (✉)
Department of Geography & the Environment, Villanova
University, Villanova, PA 19085, USA
e-mail: Nathaniel.weston@villanova.edu

S. C. Neubauer
Baruch Marine Field Laboratory, University of South
Carolina, Georgetown, SC 29442, USA

Present Address:
S. C. Neubauer
Department of Biology, Virginia Commonwealth
University, Richmond, VA 23284, USA

D. J. Velinsky
Department of Biodiversity, Earth and Environmental
Science, The Academy of Natural Sciences of Drexel
University, Philadelphia, PA 19103, USA

M. A. Vile
Department of Biology, Villanova University, Villanova,
PA 19085, USA

oligohaline site (>80 g C–CH_4 m^{-2} year^{-1}), making this site a significant GHG source ($>2,000$ g $CO_{2\text{-eq}}$ m^{-2} year^{-1}). The oligohaline site did not accumulate C over the 2 year study period, though ^{210}Pb dating indicated long term C accumulation (250 g C m^{-2} year^{-1}), suggesting seasonal salt-water intrusion can significantly alter C cycling and GHG exchange dynamics in tidal marsh ecosystems.

Introduction

Tidal marshes are among the world's most productive ecosystems (Odum 1988; Mcleod et al. 2011). The annual growth of plants within tidal marshes produces large standing stocks of biomass that reflect significant photosynthetic uptake of atmospheric carbon dioxide (CO_2). While a large portion of the plant gross primary production is respired to CO_2 or methane (CH_4) via total ecosystem respiration (ER), a fraction of the organic matter escapes decomposition and is sequestered in marsh soils. The development and expansion of tidal marshes over the past approximately 4,000 years has produced large quantities of organic rich soils (Redfield 1965), and tidal marshes may currently be an important carbon sink acting to reduce atmospheric greenhouse gas concentrations and radiative forcing (Mcleod et al. 2011; Mitsch et al. 2013). There has been discussion within the scientific and management communities of recognizing the carbon (C) sequestered in tidal marshes to enhance the economic incentives for marsh preservation and restoration (Mcleod et al. 2011; Chmura 2013) and better accounting of coastal wetland greenhouse gas dynamics in national greenhouse gas inventories (IPCC 2014).

Much of our knowledge about C cycling in tidal marshes has been attained through studies in salt marsh systems (e.g. Chmura et al. 2003). In many coastal systems, however, tidal freshwater (average salinities <0.5) and oligohaline (average salinities 0.5–5.0) marshes are found in the upper portion of the tidally influenced estuary and can account for a significant fraction of the total tidal marsh area (Odum

1988), yet relatively less is known about these types of marshes (Barendregt et al. 2009). The dominant plant types and relative importance of microbial decomposition pathways vary along salinity gradients in tidal marsh ecosystems. Characteristically, salt marshes in the U.S. are dominated by only one or two macrophyte species (often *Spartina alterniflora* and/or *S. patens*), whereas dozens of plant types can be found in tidal freshwater marshes (Neubauer et al. 2000). Tidal freshwater and oligohaline marshes can be as or more productive than salt marshes, and provide many of the same ecosystem services, including the removal of atmospheric CO_2 through the accumulation of organic C in marsh soils (Barendregt et al. 2009). Methane (CH_4) fluxes, however, are often higher from freshwater and oligohaline wetlands than from salt marshes (Bartlett et al. 1987; Poffenbarger et al. 2011). In salt marshes, seawater supplies abundant sulfate (SO_4^{2-}) which can be used by microbial sulfate reducers during the anaerobic respiration of organic matter. The higher energy yield of sulfate reduction typically results in the inhibition of methanogenesis in salt marsh soils and low CH_4 production and efflux. CH_4 is a potent greenhouse gas with a global warming potential equivalent to 25 times that of CO_2 over 100 years (Forster et al. 2007). Even modest CH_4 release can therefore largely offset short-term CO_2 uptake and sequestration in freshwater wetland soils (Whiting and Chanton 2001). While exchange of C (CO_2 and CH_4) between marsh ecosystems and the atmosphere has received attention in salt marsh systems, we know relatively less about C cycling in tidal freshwater and oligohaline marshes.

Coastal marshes, at the land-sea interface, are experiencing deviations in many environmental drivers linked to both climate change and land use change. Our understanding of the impacts of climate change and land use change on marshes remains limited (i.e., Kirwan and Megonigal 2013). Climate change is accelerating rates of sea-level rise and will alter temperature and patterns of precipitation in watersheds, influencing rates and timing of freshwater discharge to coastal systems (Smith et al. 2005; Milly et al. 2005). Land use change is further altering the supply of water, nutrients, and sediments to coastal systems (Deegan et al. 2012; Syvitski et al. 2009; Weston 2014). Changes in flooding frequency, salinity distribution, temperature, and other global change factors may directly alter carbon cycling, and long-

term changes in the distribution of tidal marshes along estuarine salinity gradients will further influence rates of CO_2 and CH_4 exchange between marshes and the atmosphere.

Salt-water intrusion has the capacity to exert especially powerful controls on marsh carbon cycling by causing disturbance to plant communities (Pezeshki et al. 1987; McKee and Mendelssohn 1989; Spalding and Hester 2007; Krauss et al. 2012; Noe et al. 2013) and altering pathways of microbial organic carbon decomposition (Weston et al. 2006, 2011; Neubauer 2013; Chambers et al. 2013; Neubauer et al. 2013). Ecosystem responses to increased salinity, however, are conflicting. For instance, Weston et al. (2011) found that saltwater intrusion resulted in greater rates of microbial organic matter decomposition and, surprisingly, higher CH_4 production and efflux from tidal freshwater marsh soils. In contrast, Neubauer (2013) observed a decline in ecosystem productivity with saltwater intrusion, but organic matter decomposition did not increase and CH_4 fluxes also declined. Our understanding of changes in marsh C cycling in response to saltwater intrusion remains limited. Changes in coastal wetland C cycling in response to saltwater intrusion will influence the ability of marshes to keep pace with sea-level rise, and may produce feedbacks to the climate system through changes in CO_2 and CH_4 exchange (Weston et al. 2011).

In this study, we evaluated C cycling in marshes along the estuarine salinity gradient in the Delaware River Estuary, situated on the mid-Atlantic coast of the United States. C cycling in a tidal freshwater marsh and a mesohaline marsh were contrasted, and the role of seasonal salt-water intrusion into an oligohaline marsh was evaluated. Four years of field gas flux measurements were used to determine patterns of gross ecosystem production (GEP), ecosystem respiration to CO_2 (ER_{CO_2}) and CH_4 (ER_{CH_4}), and net ecosystem production (NEP) to evaluate the carbon source/sink status of tidal marshes along the salinity gradient in the Delaware River Estuary. Modeled rates of C sequestration were compared to long-term measurements of C accumulation from ^{210}Pb and ^{137}Cs radiodating of marsh soils. Rates of sulfate reduction and methanogenesis were measured to determine the relative importance of these microbial organic matter decomposition pathways to net C
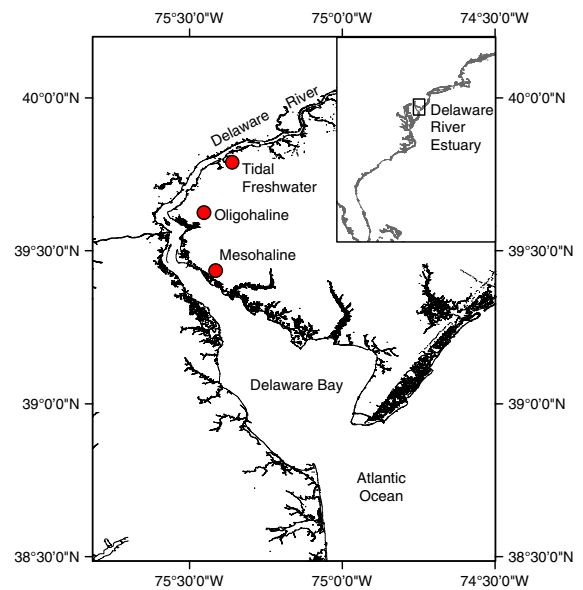
Fig. 1 Map of the Delaware River Estuary with the three study sites along the salinity gradient of the estuary indicated. The *inset* map indicates the study region on the mid-Atlantic coast of the United States

exchange. The greenhouse gas (GHG) source/sink status of each marsh type was assessed.

Methods

Study sites and monitoring

Three study sites (tidal freshwater marsh, oligohaline marsh, and mesohaline marsh) were established along the salinity gradient in Delaware River Estuary (Fig. 1). All sites were located along relatively small tidal rivers within 8 km of the main-stem of the Delaware River. The tidal freshwater marsh site (39.789745N, 75.357335W) sits along Raccoon Creek in the lower tidal freshwater portion of the estuary near Bridgeport, NJ, and is dominated by a mixed community of freshwater plants including *Peltandra virginica*, and species of *Bidens*, *Amaranthus* and *Polygonum*. The oligohaline site (39.624341N, 75.452013W) is within Mannington Township, NJ and is dominated by *Zizania aquatica* (wild rice) which forms monospecific stands at this site. The mesohaline site (39.432621N, 75.413376W) is situated along Stow Creek in the upper Delaware Bay. *S. alterniflora* is dominant at the

mesohaline site, although there is some growth of *Amaranthus cannabinus* as well.

A conductivity, salinity, and depth meter (Schlumberger CTD diver) was deployed in the tidal river through the growing season (approximately May through September) at each site in 2007, 2008 and 2009. Sites were not instrumented in 2006. A separate air temperature and pressure meter (Schlumberger baro-diver) was also deployed at each site. Because temperature was not recorded continuously at the sites and PAR was not measured, temperature and photosynthetically-active radiation (PAR) data on 15 min intervals were obtained from the Jacques Cousteau National Estuarine Research Reserve which is 60–95 km from the research sites (data available through the National Estuarine Research Reserve Centralized Data Management Office; http://cdmo.baruch.sc.edu). Delaware River discharge data at Trenton, NJ were obtained from the United States Geological Survey (site 01463500; http://waterdata.usgs.gov/usa/nwis/uv?01463500).

Field Gas Flux

At each site, six permanent sampling plots were established within the marsh platform in early spring (2006 at the tidal freshwater and mesohaline sites and 2007 at the oligohaline site) approximately 20 m from the tidal river. Square open-top collars ($0.372 \, \text{m}^2$) constructed of high density polyethylene were pushed into the marsh to a depth of approximately 0.4 m with approximately 0.1 m remaining above the surface. Holes in the collars both below-ground and above-ground (just above the soil surface) allowed for drainage and pore-water exchange. A boardwalk was constructed at each site to allow access to the plots without disturbing the surrounding marsh.

The field sites were visited periodically for measurement of CO_2 and CH_4 gas exchange rates and plant biomass. During gas flux measurements, above-ground holes in the collars were plugged with rubber stoppers and clear acrylic chambers (61 cm high with a volume of 226.5 L) were placed on the collars to form a gas-tight seal. Open-top chamber extensions were used when biomass within the plots required additional chamber height. To obtain CO_2 exchange rates, a PP Systems EGM-4 infrared gas analyzer was connected to the chamber in flow-through mode to continuously monitor CO_2 concentrations within the chamber. The change in CO_2 over time was determined within the chamber over an approximately twenty-minute period under four different light levels (100, 50, 25 and 0 % ambient light) achieved with shade cloths and reflector blankets. A probe containing both a PAR and a temperature sensor was mounted within the chamber to record environmental conditions during the gas flux measurements. CO_2 exchange measurements were conducted primarily in the growing season but several measurements were made during colder months to obtain full annual cycles of gas exchange. Measurements were conducted on 28 dates at the tidal freshwater site, 20 dates at the oligohaline site, and 27 dates at the mesohaline site.

CH_4 exchange measurements were conducted starting in 2007 (24 dates at the tidal freshwater site, 20 dates at the oligohaline site, and 23 dates at the mesohaline site). Gas samples from within the chambers were taken at the beginning, middle and end of the overall CO_2 sampling period using a 60 ml syringe and injected into evacuated 20 ml headspace vials which were returned to the laboratory. CH_4 concentrations were determined by flame ionization detector gas chromatography (Agilent 6890N), and the change in CH_4 over time was used to calculate the flux of CH_4 between the marsh and atmosphere. We assumed that over these short timescales, differences in light did not influence fluxes of CH_4 (Neubauer et al. 2000).

Respiration, primary production, and photosynthetic efficiency

Rates of ER with CO_2 and CH_4 as the product (ER_{CO_2} and ER_{CH_4}, respectively), GEP, and photosynthetic efficiency (α) were calculated from measured rates of CO_2 and CH_4 exchange using short duration static chamber incubations (Whiting et al. 1992; Weider et al. 2009). ER_{CO_2} was defined as the rate of dark CO_2 exchange, and ER_{CH_4} as the rate of CH_4 exchange. GEP was calculated from the rate of CO_2 exchange at each light level correcting for ER_{CO_2}. Photosynthetic efficiency [α; mmol C mol PAR^{-1}] was then determined from the linear relationship between GEP and PAR. Note that non-linear relationships between PAR and GEP were explored but did not improve the fit to the data (R^2 values were typically >0.95), and GEP measurements were made when PAR values were close to maximum values for that time of year.

Table 1 Linear allometric relationships between total plant stem height (cm) and dry biomass (gram dry weight; gdw) for plants harvested from tidal freshwater, oligohaline, and mesohaline sites in the Delaware River Estuary along the mid-Atlantic coast of the U7S

Plant	Site(s)	Allometric relationship		
		gdw cm^{-1}	R^2	n
Peltandra virginica	Tidal freshwater	0.018	0.64	68
Bidens	Tidal freshwater	0.190	0.94	4
Nuphar lutea	Tidal freshwater	0.053	0.80	92
Amaranthus rudis	Tidal freshwater	0.065	0.19	14
Polygonum punctatum	Tidal freshwater	0.069	0.95	6
Polygonum sagittatum	Tidal freshwater	0.236	0.91	6
Zizania aquatica	Tidal freshwater, oligohaline	0.024	0.69	92
Spartina alterniflora	Mesohaline	0.018	0.84	82

Plant biomass

Plant biomass was measured nondestructively within each of the six permanent collars at the three sampling sites starting in 2007. The total number and height of each plant species in each collar was determined. Biomass was calculated using species-specific linear allometric relationships between stem height and biomass developed by destructive sampling of vegetation plots outside of the permanent collars (Table 1). These relationships were derived over several years and at various times during the season ($n > 60$ for dominant plant species). The stock of C in the aboveground biomass was calculated using biomass measurements and plant C content values for the dominant plant species (47.1, 41.9, 35.9, and 40.8 % C for *P. virginica*, *Bidens* spp., *Z. aquatica*, and *S. alterniflora*, respectively; Neubauer and Richardson unpublished data).

Biogeochemistry and microbial process rates

Duplicate intact soil cores ($n = 2$; 170 cm^2 surface area; depth of approximately 25 cm) were obtained from each of the marsh sites adjacent to the permanent plots on 2 dates in 2007 (July and October) and 3 dates in 2008 (April, July and October). Soil temperature profiles were obtained at the time of collection using a thermocouple probe. The soil cores were transported to the laboratory and sectioned under a N$_2$ atmosphere into 2 cm depth increments for soil biogeochemical and microbial rate measurements (Weston et al. 2006, 2011). A portion of each soil depth was centrifuged (4,500 rpm for 10 min) to obtain porewater, which was distributed into a number of separate vials and preserved according to future analysis to be performed. Porewater pH was determined immediately, and a subsample of porewater was preserved in 20 % zinc acetate for measurement of hydrogen sulfide (H$_2$S; colorimetric; Cline 1969). Phosphate (PO$_4^{3-}$; colorimetric: Murphy and Riley 1962), dissolved organic carbon (DOC; high temperature combustion on Shimadzu TOC), and chloride (Cl$^-$) and SO$_4^{2-}$ (ion chromatography on a Dionex DX-500) were measured on porewater acidified with 12.5 µl ml^{-1} of 6 N nitric acid. Ammonium (NH$_4^+$; colorimetric; Solórzano 1969) and low molecular weight organic acids (glycolate, lactate, acetate, propionate, formate, butyrate, iso-butyrate, valerate, iso-valerate and succinate analyzed by high pressure liquid chromatography following derivatization; Albert and Martens 1997) were determined on samples that had been frozen. Samples for dissolved inorganic carbon (DIC; Shimadzu TOC) were preserved with 50 µl ml^{-1} saturated mercuric chloride. Soil biogeochemical parameters were averaged by depth (to a depth of 16 cm) and reported as averages (µM) or integrated by depth (to 16 cm) and reported as inventories (mmol m^{-2}). A portion (2 cm^{-3}) of each soil section was dried (80 °C) to determine soil porosity and bulk density. Dried soil was then ground and a subsample from each depth was used for measurement of soil organic C following acidification on a Costech elemental analyzer (for July and October 2007 and October 2008 dates only).

Rates of microbial sulfate reduction, hydrogenotrophic methanogenesis, and acetoclastic methanogenesis were measured using radiotracer incubations on six depths for each soil core (0–2, 2–4, 4–6, 8–10, 12–14 and 18-20 cm). Six 2-cm^3 samples were obtained from each depth in cut-off syringes, which were stoppered and injected with 1 µCi ^{35}SO$_4^{2-}$, 1 µCi H^{14}CO$_3^-$, or 0.2 µCi ^{14}CH$_3$COOH (each in duplicate). Samples were incubated at average in situ temperatures across sites (9.5 °C in April 2008, 25 °C

in July 2007 and 2008, and 18 °C in October 2007 and 2008), so any differences between sites are due to site-specific factors and not the incubation temperature. The soils were incubated for approximately 15 h, and the radiotracer incubations were then preserved. ^{35}S soils were preserved with 10 ml of 20 % zinc acetate and frozen, and ^{14}C soils were preserved with 2 ml of 6 N HCl in gas headspace vials.

Rates of sulfate reduction were determined following cold chromium distillation of the ^{35}S soil incubations (Kallmeyer et al. 2004). The activity of the total reduced sulfur (TRS) pool was measured by liquid scintillation counting. The ^{14}C activities of CH_4 and CO_2 were determined using a purge and trap method (Weston et al. 2011) coupled to a gas chromatograph (Agilent 6890N) and a gas proportional counter (Raytest Raga Star). Rates of microbial sulfate reduction, hydrogenotrophic methanogenesis, and acetoclastic methanogenesis were calculated as follows:

$$\text{Rate} = \text{Tracer}_{\text{Product}} \times (\text{Tracer}_{\text{Substrate}})^{-1} \\ \times [\text{Substrate}] \times \varphi \times \alpha \times t^{-1}, \quad (1)$$

where tracer$_{\text{product}}$ is the activity of the product ($^{14}CH_4$ or TR^{35}S), tracer$_{\text{substrate}}$ is the activity of the tracer added (1 µCi $^{35}SO_4^{2-}$, 1 µCi $H^{14}CO_3^-$, or 0.2 µCi $^{14}CH_3COOH$, respectively), [substrate] is the concentration of the substrate (SO_4^{2-}, DIC, or acetate, respectively), φ is the soil porosity, α is the isotope fractionation factor (1.06; Jørgensen 1982; Orcutt et al. 2005), and t is the incubation time. Depth-specific rates were integrated over depth (to 16 cm) to obtain areal rates (mmol m^{-2} d^{-1}).

Net ecosystem metabolism and net atmospheric carbon exchange

To estimate total GEP, NEP, ER$_{CO_2}$, ER$_{CH_4}$, sulfate reduction, methanogenesis, and source/sink status for greenhouse gases (GHG), we constructed a simple model to evaluate these processes over daily, monthly, and annual timescales. We modeled these processes on 15 min intervals for the years 2007 and 2008, when the most comprehensive measurements were taken. Each plot was modeled separately to obtain estimates of variability at each site. Note that PAR (for GEP) and temperature (for ER$_{CO_2}$ and ER$_{CH_4}$) were used only to model fluctuations in GEP, NEP, ER$_{CO_2}$, and ER$_{CH_4}$ from measured rates of these processes to account for

changes on daily timescales of both light and temperature and between sampling dates (i.e., cloudy days and warm/cold fronts). The overall seasonal patterns of these processes were derived for each plot directly from the field measurements, and the interpolation between these plot-level measurements was simply corrected using the PAR and temperature model. This approach retains the variability between plots (as each was modeled separately) and more directly accounts for changes in the metabolic processes driven by, for instance, plant phenology rather than directly by light and/or temperature.

GEP was calculated from photosynthetic efficiency (α) and PAR. α was determined from the relationship between GEP and PAR for each sampling plot for each sampling date and interpolated over time. Using PAR on 15 min intervals, the GEP for each interval was then

$$GEP = \alpha \times PAR \quad (2)$$

For ER$_{CO_2}$, the measured rate of respiration to CO_2 on each sampling date for each plot was used as a baseline rate of ER$_{CO_2}$ (ER$_{CO_2(B)}$) at the temperature during sampling (baseline temperature; T$_B$) and this was interpolated between sampling dates for each plot separately. Flooding was assumed not to affect ER$_{CO_2}$ based on previous measurements of respiration in tidal marsh systems (Neubauer et al. 2000). The response of respiration to temperature was determined separately for each plot using the Arrhenius equation (Westrich and Berner 1988) to derive the activation energy (E$_a$; kJ mol^{-1}):

$$ER_{CO_2} = Ae^{\left(-\frac{E_a}{RT}\right)} \quad (3)$$

where A is a constant, R is the gas constant, and T is temperature. The rate of ER$_{CO_2}$ at any given 15 min interval was then a function of the interpolated ER$_{CO_2(B)}$ corrected for the deviation in measured temperature from T$_B$.

ER$_{CH_4}$ was calculated in a similar manner, with a combination of interpolation and temperature correction using the Arrhenius equation except at the mesohaline site where there was not a significant relationship between temperature and ER$_{CH_4}$ and ER$_{CH_4}$ was therefore simply interpolated between sampling dates without correction for temperature. Flooding has been shown to influence CH_4 flux from tidal marsh soils (Neubauer et al. 2000). ER$_{CH_4}$ was

measured only during exposed conditions in this study ($ER_{CH_4 \ (exposed)}$) and a correction factor was applied to ER_{CH_4} during inundated conditions (0.12; $ER_{CH_4(inundated)}$) based on previous comparisons of CH_4 fluxes in tidal marsh systems (Neubauer et al. 2000) and using the measured frequency of marsh inundation at each site (f):

$$ER_{CH_4} = \left[(1-f) \times ER_{CH_4(exposed)} \right] \\ + \left[f \times 0.12 \times ER_{CH_4(exposed)} \right] \quad (4)$$

NEP was then calculated as the net of carbon uptake and release processes:

$$NEP = GEP - ER_{CO_2} - ER_{CH_4}, \quad (5)$$

where negative NEP signifies the marsh is a net C source to the atmosphere, and positive NEP corresponds to marsh uptake of C. Note that the NEP term only includes exchange with the atmosphere and is not the same as the ecosystem carbon balance; lateral inputs (such as sequestration of C deposited in settling suspended sediment) and outputs (such as erosion or effluxes of dissolved organic carbon into tidal water) are not considered here. Finally, the net greenhouse gas (GHG) exchange of each plot was calculated on a CO_2-equivalence basis assuming a 100 year global warming potential (GWP) of 25 for CH_4:

$$GHG = ER_{CO_2} + 25(ER_{CH_4}) - GPP, \quad (6)$$

where positive GHG denotes that the marsh is a source of GHG to the atmosphere.

Rates of sulfate reduction, hydrogenotrophic methanogenesis, and acetoclastic methanogenesis over an annual cycle were estimated from the relationship between each process rate and temperature and porewater Cl^- inventories across all three sites. Daily values for porewater Cl^- inventories during 2007 and 2008 were derived from the site-specific relationship between measured porewater Cl^- at each site and conductivity in the overlying water determined from field site monitoring (average conductivity over the prior 2 months was found to give the best prediction). For dates when overlying water conductivity was not available, the site-specific relationship between conductivity and river discharge was used to estimate conductivity (again a 2 month prior average discharge was found to produce the closest fit to measured conductivity). Respiration via sulfate reduction and acetoclastic methanogenesis (ER_{SR} and ER_{MG},

respectively) were calculated on a per C basis assuming 2 CO_2 per sulfate reduced and 2 C (1 CO_2 and 1 CH_4) per acetate disproportionated (Vile et al. 2003).

The calculated rates of GEP, ER_{CO_2}, ER_{CH_4}, NEP, GHG, ER_{SR}, and ER_{MG} were integrated over two years (2007 and 2008) to obtain monthly and annual estimates of processes. The relative importance of plant respiration processes to the overall ER (f_{Plant}) was estimated by assuming plants respired between 40 and 50 % of the C they fix through GEP in both salt marshes (Dai and Wiegert 1996) and tidal freshwater marshes (Neubauer et al. 2000). The relative contribution of sulfate reduction and acetoclastic methanogenesis to total ER (f_{SR} and f_{MG}, respectively) was also estimated.

Long-term carbon accretion

Historical rates of C accretion in marsh soils at the three sites were determined by combining measurements of marsh accretion with soil C content. Rates of marsh accretion were measured by ^{210}Pb and ^{137}Cs radiodating of marsh soil cores. Soil cores were obtained to a depth of 80 + cm at each site in early 2008, sectioned into 1, 2, or 4 cm intervals (interval increased with depth), and analyzed by gamma spectroscopy (Canberra Broad Energy Germanium Detector). ^{210}Pb and ^{137}Cs activities were measured at 46.5 and 661.6 keV, respectively. The constant rate of supply (CRS) model (Oldfield and Appleby 1984; Craft and Richardson 1998) was used to calculate accretion rates using ^{210}Pb activities, and vertical accretion above the depth at which ^{137}Cs was not detected was defined as accretion since 1958 (Ritchie and McHenry 1990). C accretion (g C m^{-2} year^{-1}) was calculated using both ^{210}Pb and ^{137}Cs accretion rates (cm year^{-1}), average soil organic C at each site (g C g^{-1}), and average dry bulk density at each site (g dry sediment cm^{-3}).

Statistical analyses

The peak values for aboveground biomass, α, ER_{CO_2}, and ER_{CH_4} were determined for each plot ($n = 6$ plots per site) during each year ($n = 3$ or 4 years depending on variable and site), and differences in these measured field variables between sites ($n = 3$ sites)

were evaluated using a repeated measures analysis of variance (rmANOVA). Select contrasts between years within a single site were assessed using a one-way analysis of variance (ANOVA). Similarly, differences in biogeochemical variables (Cl^-, SO_4^{2-}, DIC, DOC, NH_4^+, PO_4^{3-}, H_2S, acetate, LMW-OAs, pH, porosity, bulk density, and organic C) between sites ($n = 3$ sites) from duplicate soil cores ($n = 2$ cores per site per date) taken on five sampling dates were evaluated with rmANOVA tests. Differences in modelled annual rates of GEP, NEP, ER_{CO_2}, ER_{CH_4}, and GHG between sites ($n = 6$ plots per site) were similarly determined using rmANOVA. Significant differences between sites for all ANOVA and rmANOVA tests were evaluated with Tukey's post hoc tests.

To evaluate seasonal and spatial patterns in biogeochemistry and microbial rates, soil inventories of all biogeochemical parameters and process rates were regressed against both porewater inventories of Cl^- (as a proxy for salinity) and temperature in a multiple linear regression using data across all three sites concurrently. Multiple linear regressions were employed with Cl^- inventories and temperature as independent variables in a backwards stepwise fashion (variable removed if $p > 0.05$) to predict biogeochemistry and microbial rates. Statistical analyses were performed in SPSS version 21 (IBM Corporation).

Results

Field site monitoring

Field monitoring of the study sites indicated a clear gradient of salinity down-estuary, with seasonal signals and interannual variability (Fig. 2). The tidal freshwater site was mostly fresh, but experienced slight increases in average daily salinity in 2007 and 2008 (but not in 2009) during late summer and early fall following sustained periods of low discharge from the Delaware River in these years (Fig. 2). Conductivity at the oligohaline site indicated that this site was fresh in the spring and became slightly saline in the late summer and early fall, with maximum conductivities of about 10 mS cm^{-1} (corresponding to salinities of about 5.5) in 2007 and 2008, but maximum conductivity was notably lower in 2009. No freshwater conditions were observed at the mesohaline site,

and conductivities of about 24 mS cm^{-1} were observed in late summer and early fall (corresponding to salinities of approximately 14.5; Fig. 2). Note that late summer (August) conductivities were substantially lower at all sites in 2009 than in the preceding two years due to a higher frequency of low volume summer discharge events in 2009 that increased the average discharge in late summer well above the long-term average (Fig. 2).

Monitoring of water level on the marsh surface at each site indicated that average daily maximum flooding depth was similar between the three sites (45.7 cm at the tidal freshwater site, 57.0 cm at the oligohaline site, and 58.6 cm at the mesohaline site), as was the average duration of marsh flooding (47, 55, and 37 %, respectively).

Biomass and flux measurements

Plant biomass, ER_{CO_2}, ER_{CH_4}, and α exhibited clear seasonal patterns with low values in the winter months and peak values in the summer and early fall (Fig. 3). Monospecific stands of *Z. aquatica* and *S. alterniflora* were observed in the plots at the oligohaline and mesohaline sites, respectively, throughout the study period, reaching peak biomass values generally in excess of 400 g m^{-2} (Table 2). *P. virginica* was the dominant plant at the tidal freshwater marsh site and exhibited relatively stable biomass over the three years, though a mixed freshwater community including *Bidens*, *Amaranthus* and *Polygonum* developed later in the summer and was more variable from year to year. Note that peak aboveground biomass of *Z. aquatica* was reached in early August at the oligohaline site followed by rapid biomass decline, markedly earlier than fall biomass declines at the tidal freshwater and mesohaline sites (Fig. 3). There were significant differences between sites for peak biomass in specific years (for instance, the tidal freshwater marsh had the highest biomass in 2007; Table 2; ANOVA, $F_{(2,15)} = 28.2$; $p < 0.001$) but variability between years resulted in no significant overall between-site differences in peak annual biomass (rmANOVA $F_{(2,51)} = 2.23$, $p = 0.142$). There was a significant negative correlation ($p < 0.001$) between peak aboveground biomass and the average water-column conductivities over the prior month at the oligohaline and mesohaline sites (Fig. 4).
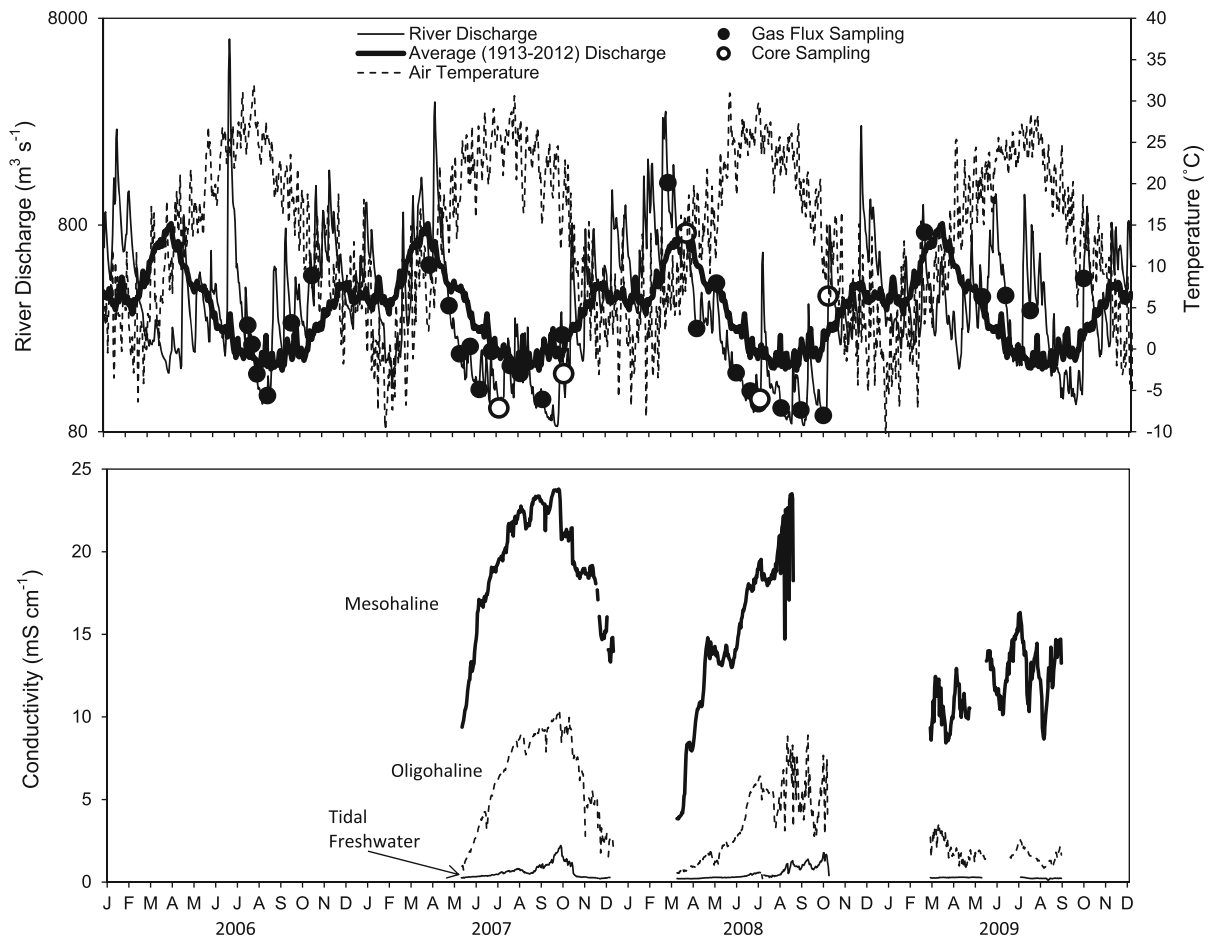
Fig. 2 (*top*) Delaware River discharge (USGS station 01463500; Delaware River at Trenton, NJ; http://waterdata.usgs.gov/usa/nwis/uv?01463500), average daily discharge (100 years record), and air temperature during the study period with gas flux and core sampling dates indicated, and (*bottom*) average daily water-column conductivities at the three sampling sites

Peak α was marginally significantly different between sites (rmANOVA $F_{(2,13)} = 3.62$; $p = 0.052$) with a significantly higher α at the tidal freshwater site than the mesohaline site (Tukey post hoc $p < 0.05$; Table 2; Fig. 3). Aboveground biomass production and peak photosynthetic efficiency were significantly related across all sites (Table 2; $\alpha = 0.02 \times$ biomass $+ 4.45$; $R^2 = 0.75$; $p = 0.002$).

Peak annual ER_{CO_2} was significantly different between sites (rmANOVA $F_{(2,13)} = 7.48$, $p = 0.006$), with higher ER_{CO_2} in the oligohaline marsh than at the mesohaline site (Tukey post hoc, $p < 0.05$; Table 2; Fig. 3). Mean peak ER_{CO_2} in the tidal freshwater marsh was not significantly different than the other two sites (Tukey post hoc, $p > 0.05$) as there

was substantial year to year variability in peak ER_{CO_2} (Table 2). Peak ER_{CO_2} was greater in 2007 than in other years at the tidal freshwater site (ANOVA $F_{(3,20)} = 17.6$; $p < 0.001$). ER_{CO_2} at each site was significantly ($p < 0.001$), positively related to temperature (Fig. 5).

Peak ER_{CH_4} was significantly different between sites (rmANOVA $F_{(2,13)} = 10.72$; $p = 0.002$), with the oligohaline marsh exhibiting significantly higher ER_{CH_4} than the other two sites (Table 2; Tukey post hoc; $p < 0.05$). ER_{CH_4} was lower at the tidal freshwater site, and there was overall net CH_4 consumption in the mesohaline salt marsh site, though there was not a significant difference between these two sites (Tukey; $p > 0.05$; Fig. 3). ER_{CH_4} was significantly correlated
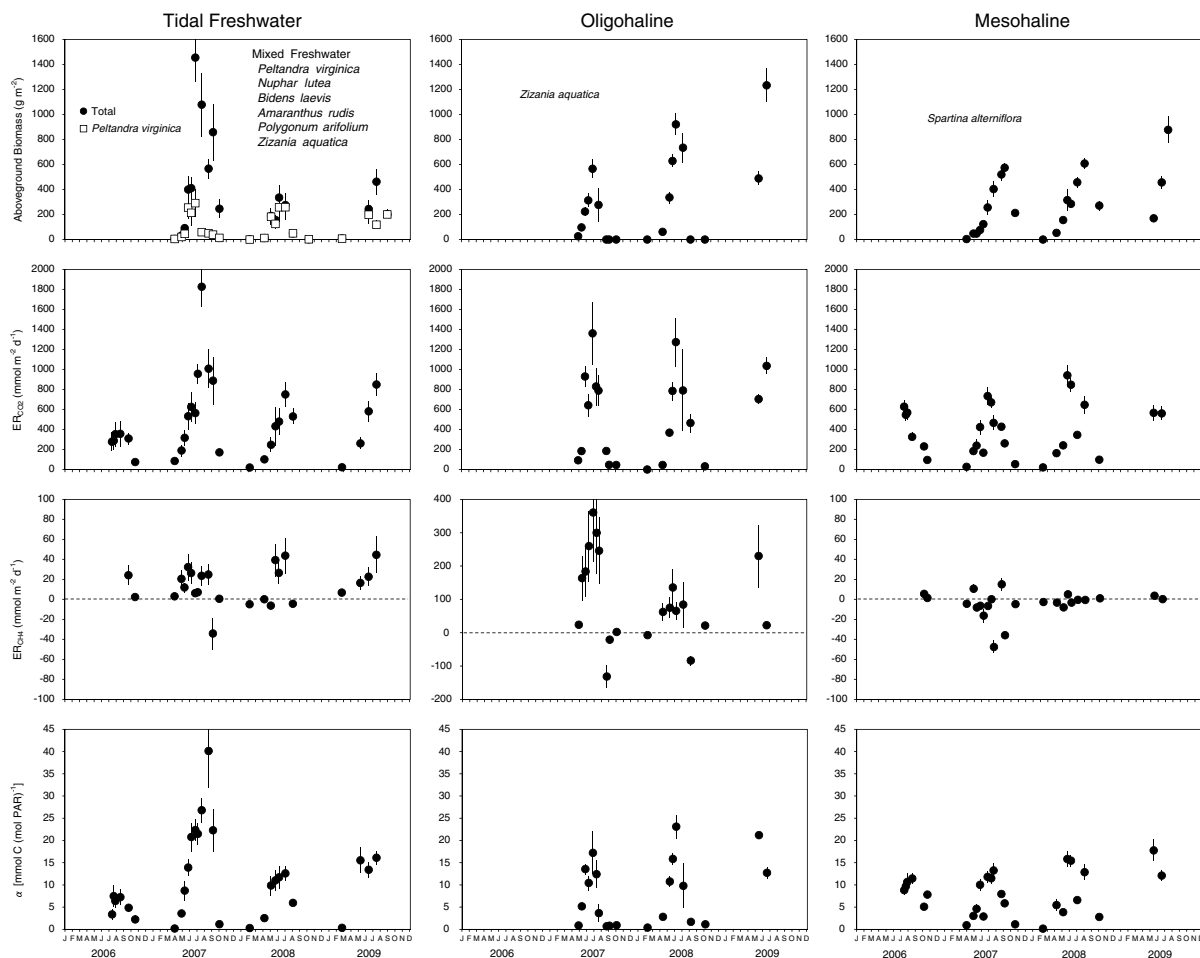
Fig. 3 Aboveground biomass, ecosystem respiration to CO_2 (ER_{CO_2}) and CH_4 (ER_{CH_4}) and photosynthetic efficiency (α) at the three study sites over 4 years. The plant species are noted in the aboveground biomass panels, and for the tidal freshwater site the *Peltandra virginica* aboveground biomass and the total aboveground biomass (including *P. virginica*) are shown. Note the change in scale on ER_{CH_4} panels

with temperature at the tidal freshwater and olighaline sites ($p < 0.001$), but there was no significant relationship between temperature and CH_4 flux in the mesohaline marsh ($p > 0.05$; Fig. 5).

Biogeochemistry and microbial process rates

There were significant differences between soil porewater concentrations of Cl^-, SO_4^{2-}, DIC, NH_4^+, PO_4^{3-}, H_2S, and LMW-OAs, (Table 3) and rates of sulfate reduction and acetoclastic methanogenesis (Table 4) between sites (rmANOVA $p < 0.05$). Cl^-, SO_4^{2-}, and H_2S were highest at the mesohaline site (Table 3). DIC, NH_4^+, and PO_4^{3-} were lowest at the

tidal freshwater site. LMW-OAs were highest at the tidal freshwater and oligohaline sites. There were no significant differences in DOC and acetate between sites (Table 3). Rates of sulfate reduction were significantly higher at the mesohaline salt marsh site than the other two sites, while rates of acetoclastic methanogenesis were higher at the tidal freshwater marsh site than the other sites (Table 4). Rates of hydrogenotrophic methanogenesis were quite low compared to the other measured microbial pathways and did not differ significantly between sites (Table 4).

There were significant seasonal differences in porewater Cl^- concentrations at each of the sites

Table 2 Aboveground biomass production, peak photosynthetic efficiency (α), peak ecosystem respiration to CO_2 (ER_{CO2}) and CH_4 (ER_{CH_4}; mean $\pm$ 1 SD from 6 plots) during 4 years at tidal freshwater, oligohaline, and mesohaline sites along the estuarine salinity gradient in the Delaware River Estuary

Site	Year	Aboveground Biomass Production (gdw m^{-2} year^{-1})	Peak α (mmol C mol PAR^{-1})	Peak ER_{CO2} (mmol C m^{-2} d^{-1})	Peak ER_{CH_4} (mmol C m^{-2} d^{-1})
Tidal fresh: *Peltandra virginica* mixed community	2006	ND	9.4 $\pm$ 5.4	441.5 $\pm$ 291.1	24.2 $\pm$ 9.6
	2007	1559.1 $\pm$ 407.5	42.0 $\pm$ 17.5	1837.5 $\pm$ 487.1	62.4 $\pm$ 40.4
	2008	363.8 $\pm$ 225.2	14.3 $\pm$ 4.2	760.1 $\pm$ 322.3	69.7 $\pm$ 28.3
	2009	514.8 $\pm$ 231.0	17.9 $\pm$ 4.3	856.5 $\pm$ 262.7	46.7 $\pm$ 21.9
	Average	812.6 $\pm$ 615.3	20.9 $\pm$ 15.7	973.9 $\pm$ 625.8	50.7 $\pm$ 31.2
	Rank		B	AB	A
Oligohaline: *Zizania aquatica*	2006	ND	ND	ND	ND
	2007	566.4 $\pm$ 182.0	19.2 $\pm$ 9.7	1490.6 $\pm$ 569.5	503.4 $\pm$ 475.2
	2008	951.7 $\pm$ 175.6	23.8 $\pm$ 6.3	1534.0 $\pm$ 540.8	194.4 $\pm$ 110.3
	2009	1233.1 $\pm$ 332.4	16.9 $\pm$ 4.9	1035.5 $\pm$ 197.5	186.1 $\pm$ 144.0
	Average	917.1 $\pm$ 361.1	20.0 $\pm$ 7.4	1353.4 $\pm$ 496.7	272.7 $\pm$ 325.4
	Rank		AB	B	B
Mesohaline: *Spartina alterniflora*	2006	ND	13.9 $\pm$ 2.5	639.2 $\pm$ 153.6	13.1 $\pm$ 27.3
	2007	578.7 $\pm$ 87.8	15.4 $\pm$ 2.6	773.0 $\pm$ 158.8	32.8 $\pm$ 15.3
	2008	634.7 $\pm$ 113.2	16.7 $\pm$ 4.0	956.1 $\pm$ 245.1	11.1 $\pm$ 9.3
	2009	456.0 $\pm$ 127.1	16.8 $\pm$ 5.8	643.5 $\pm$ 140.5	3.3 $\pm$ 4.9
	Average	556.5 $\pm$ 129.2	15.7 $\pm$ 3.9	752.9 $\pm$ 212.9	15.1 $\pm$ 19.0
	Rank		A	A	A
	F	2.23	3.62	7.48	10.72
	p	0.142	0.052	0.006	0.002

The overall average across all years is given, and rank denotes significant differences between sites (sites that do not share the same letter are significantly different; Tukey post-hoc; $p < 0.05$) based on a repeated measures analysis of variance (F statistic and p values are given at bottom)
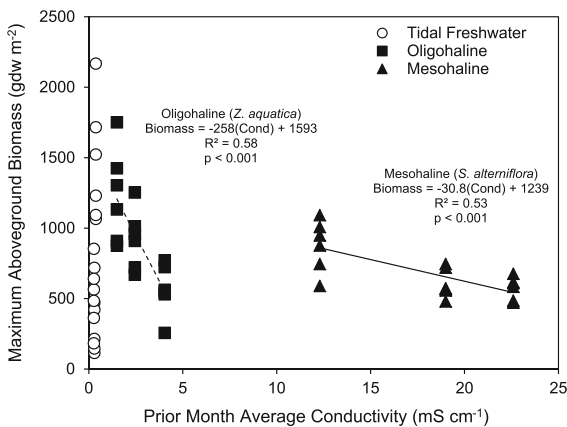
Fig. 4 Relationships between peak aboveground biomass and average water-column conductivities for the month prior to peak biomass at three study sites over three years (2007–2009). Best-fit linear regressions are shown for the oligohaline and mesohaline sites

(ANOVA $F_{(4,5)}$ = 11.8, 15.7, and 21.2 at the tidal freshwater, oligohaline, and mesohaline sites, respectively; all $p < 0.01$) with the lowest Cl^- observed during spring and highest in the fall (Table 3) that mirrored changes in the overlying water conductivity at each site (Fig. 2). To evaluate seasonal and spatial patterns in biogeochemistry and microbial rates, these measurements were regressed against porewater inventories of Cl^- (as a proxy for salinity) and temperature across all three sites simultaneously (Table 5). DIC and H_2S were significantly, positively correlated with porewater Cl^- inventories, and DOC was positively correlated with temperature ($p < 0.05$; Table 5). PO_4^{3-} inventories increased with Cl^- but declined with temperature. Both acetate and LMW-OAs were negatively correlated with Cl^- but increased with temperature across all three sites ($p < 0.05$; Table 5). Rates of all measured microbial
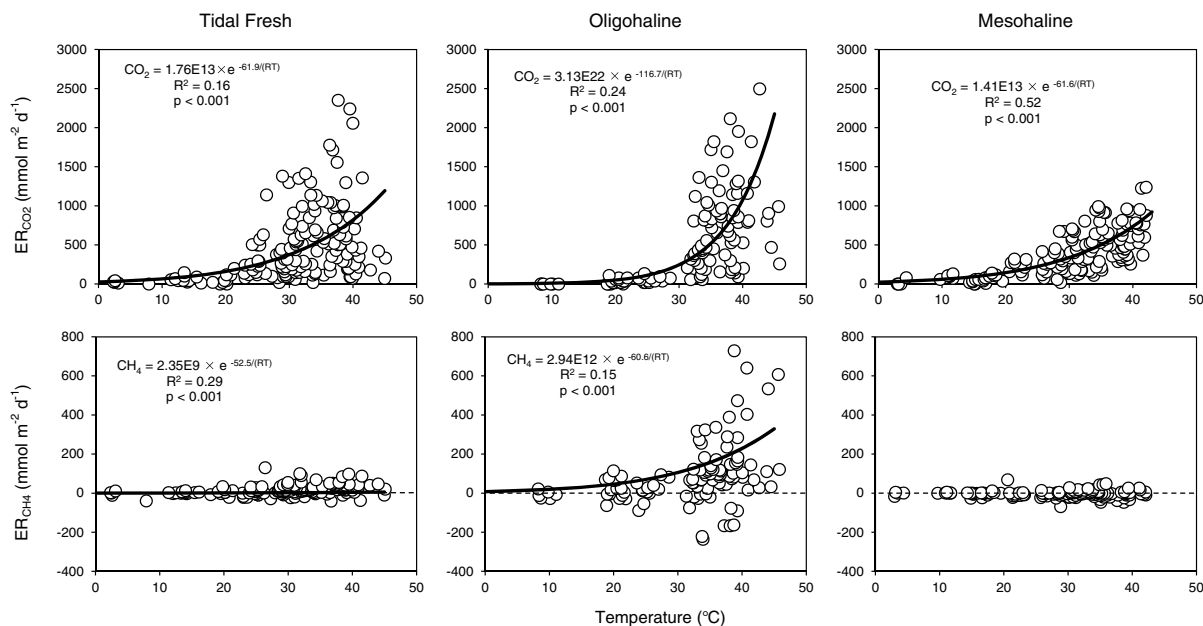
Fig. 5 The relationships between (*top*) temperature and ecosystem respiration to CO_2 (ER_{CO_2}) and (*bottom*) temperature and ecosystem respiration to CH_4 (ER_{CH_4}). Significant regressions ($p < 0.05$; Eq. 3) are indicated

processes were significantly positively correlated with temperature, and sulfate reduction was also significantly correlated with Cl^- while both pathways of methanogenesis were negatively correlated with Cl^- ($p < 0.05$; Table 5).

Ecosystem production and greenhouse gas exchange model

Modeled rates of average monthly GEP, ER_{CO_2}, ER_{CH_4}, and NEP demonstrated clear seasonal patterns (Fig. 6), with higher rates in summer and early fall and lower rates in the winter. GEP at the oligohaline site declined earlier in the year compared to the tidal freshwater and mesohaline sites (Fig. 6), reflecting the decline in *Z. aquatica* biomass in early August (Fig. 3). On an annual basis, GEP was significantly higher at the tidal freshwater marsh than the other sites (rmANOVA $F_{(2,15)} = 7.59$; $p = 0.005$; Tukey post hoc $p < 0.05$), largely due to high annual GPP during 2007 (Fig. 7). ER_{CO_2} followed a seasonal pattern similar to GEP with peak values in July or August (Fig. 6). As with GEP, the tidal freshwater site had the highest rate of ER_{CO_2} on an annual basis (rmANOVA $F_{(2,15)} = 7.51$; $p = 0.005$; Tukey post hoc $p < 0.05$), again due to high ER_{CO_2} in 2007 at this site (Fig. 7).

Note that ER_{CO_2} at the tidal freshwater site remained higher than the other sites in the fall and into early winter (Fig. 6). Annual ER_{CH_4} was significantly different between sites (rmANOVA $F_{(2,15)} = 9.17$; $p = 0.002$) with higher values at the oligohaline site than at either of the other sites (Fig. 7; Tukey $p < 0.05$). ER_{CH_4} was highest in the summer growing season in the tidal freshwater and oligohaline marshes, and there was little seasonal pattern in ER_{CH_4} in the mesohaline marsh which demonstrated net CH_4 uptake for much of the two years (Fig. 6). While ER_{CH_4} was not significantly different between the tidal freshwater marsh and the mesohaline salt marsh sites in the rmANOVA including data from all three sites (Tukey $p > 0.05$; due to high variability in the oligohaline values), when these two sites were considered independently there was a significant difference (rmANOVA $F_{(1,10)} = 8.85$; $p = 0.019$) with lower ER_{CH_4} at mesohaline sites than at the tidal freshwater site.

NEP exhibited a seasonal pattern with net C uptake in the spring at all sites (Fig. 6). The mesohaline site remained a C sink throughout the growing season, while the tidal freshwater and oligohaline sites released C during the late summer and fall, though note there was a marked difference in the NEP

Table 3 Marsh soil porewater concentrations of chloride (Cl⁻), sulfate (SO_4^{2-}), dissolved inorganic carbon (DIC), dissolved organic carbon (DOC), ammonium (NH_4^+), phosphate (PO_4^{3-}), hydrogen sulfide (H_2S), acetate, and total low molecular weight organic acids (LMW-OAs), as well as porewater pH and soil porosity and dry bulk density on five sampling dates, along with soil organic C content on three dates, for 3 sites along the salinity gradient in the Delaware River Estuary. Averages (±SD) are given from 8 depth increments (2 cm each) to a depth of 16 cm in duplicate soil cores (n = 2) for each date

Date	Cl⁻ (µM)	SO_4^{2-} (µM)	DIC (µM)	DOC (µM)	NH_4^+ (µM)	PO_4^{3-} (µM)	H_2S (µM)	Acetate (µM C)
Tidal fresh								
July 2007	2573 ± 379	23.3 ± 33.4	115.7 ± 14.8	2054 ± 711	11.4 ± 6.1	20.6 ± 8.5	0.0 ± 0.0	140.7 ± 113.8
October 2007	7339 ± 2741	99.3 ± 138.3	186.3 ± 112.5	1776 ± 623	59.7 ± 38.1	25.9 ± 23.2	0.0 ± 0.0	179.2 ± 108.5
April 2008	2103 ± 785	206.2 ± 168.5	92.3 ± 5.7	2111 ± 971	7.1 ± 2.1	29.4 ± 10.5	0.0 ± 0.0	111.3 ± 91.5
July 2008	2496 ± 484	9.1 ± 7.2	297.6 ± 264.5	8964 ± 6717	17.5 ± 3.7	19.8 ± 19.8	0.0 ± 0.0	986.3 ± 652.9
October 2008	8261 ± 2343	37.8 ± 119.8	720.6 ± 530.6	1881 ± 1722	128.3 ± 80.2	47.7 ± 29.3	0.0 ± 0.0	91.2 ± 91.3
Average	4554 ± 3143	75.1 ± 131.4	282.5 ± 350.6	3357 ± 4178	44.8 ± 60.3	28.7 ± 21.9	0.0 ± 0.0	301.7 ± 454.3
Rank	A	A	A		A	A	A	
Oligohaline								
July 2007	31247 ± 5494	47 ± 85	512 ± 273	2511 ± 249	829.8 ± 215.7	170.2 ± 59.0	0.0 ± 0.0	42.7 ± 12.8
October 2007	75190 ± 14358	586 ± 839	1079 ± 406	1958 ± 214	477.5 ± 140.9	72.9 ± 85.4	0.0 ± 0.0	48.0 ± 44.9
April 2008	22640 ± 13997	8 ± 13	464 ± 147	2371 ± 726	86.3 ± 100.9	213.7 ± 43.4	0.0 ± 0.0	305.4 ± 348.8
July 2008	40358 ± 6910	109 ± 273	1254 ± 446	2333 ± 325	74.5 ± 24.9	68.3 ± 30.0	0.0 ± 0.0	152.1 ± 93.4
October 2008	56221 ± 14513	598 ± 826	5413 ± 1832	2106 ± 453	470.3 ± 120.3	182.9 ± 111.8	0.0 ± 0.0	23.1 ± 11.9
Average	44847 ± 22113	261 ± 582	1650 ± 1973	2260 ± 468	385.6 ± 316.6	140.6 ± 91.7	0.0 ± 0.0	121.2 ± 194.0
Rank	B	A	B		B	B	A	
Mesohaline								
July 2007	164804 ± 30182	5875 ± 4809	1881 ± 978	1711 ± 476	220.9 ± 160.0	127.6 ± 72.8	285 ± 371	32.6 ± 16.1
October 2007	191072 ± 28910	5997 ± 3106	3043 ± 1014	1629 ± 393	346.9 ± 160.2	108.2 ± 56.8	336 ± 278	40.5 ± 25.5
April 2008	81317 ± 22200	2302 ± 663	2050 ± 1182	1627 ± 347	156.4 ± 95.5	188.4 ± 42.8	332 ± 595	34.2 ± 36.5
July 2008	150269 ± 24664	4774 ± 1925	2703 ± 1060	6349 ± 3444	213.1 ± 98.4	92.0 ± 47.7	296 ± 345	50.5 ± 60.3
October 2008	148220 ± 35606	4350 ± 3106	3392 ± 1850	2558 ± 961	227.1 ± 174.6	162.4 ± 88.9	596 ± 896	93.8 ± 184.5
Average	147137 ± 45992	4660 ± 3264	2614 ± 1357	2775 ± 2425	235.1 ± 156.5	135.7 ± 71.8	369 ± 544	50.6 ± 90.2
Rank	C	B	B		C	B	B	
F	844.20	4057.70	47.60	1.03	108.30	60.60	104.10	8.00
p	<0.001	<0.001	0.005	0.456	<0.001	0.004	0.002	0.063

Table 3 continued

Date	LMW-OAs (µM C)	pH	Porosity	Bulk Density (g cm^{-3})	Organic C (%)
Tidal fresh					
July 2007	771 ± 274	6.39 ± 0.10	0.65 ± 0.09	0.72 ± 0.06	6.02 ± 0.86
October 2007	1348 ± 532	6.26 ± 0.17	0.62 ± 0.07	0.66 ± 0.12	6.51 ± 1.27
April 2008	391 ± 247	6.31 ± 0.09	0.60 ± 0.07	0.76 ± 0.07	ND
July 2008	1771 ± 623	6.26 ± 0.07	0.67 ± 0.07	0.69 ± 0.17	ND
October 2008	1045 ± 508	6.47 ± 0.20	0.61 ± 0.11	0.69 ± 0.20	6.35 ± 0.86
Average	1065 ± 651	6.34 ± 0.16	0.63 ± 0.09	0.70 ± 0.14	6.28 ± 1.01
Rank	B	A	A	C	B
Oligohaline					
July 2007	2246 ± 395	6.60 ± 0.06	0.77 ± 0.05	0.35 ± 0.07	4.21 ± 0.26
October 2007	683 ± 401	6.49 ± 0.10	0.80 ± 0.13	0.37 ± 0.07	4.18 ± 0.24
April 2008	900 ± 397	6.81 ± 0.16	0.76 ± 0.10	0.36 ± 0.05	ND
July 2008	1154 ± 732	6.56 ± 0.07	0.73 ± 0.10	0.36 ± 0.06	ND
October 2008	818 ± 268	6.39 ± 0.17	0.77 ± 0.12	0.31 ± 0.08	4.61 ± 0.54
Average	1161 ± 725	6.57 ± 0.18	0.77 ± 0.10	0.35 ± 0.07	4.32 ± 0.41
Rank	AB	B	B	A	A
Mesohaline					
July 2007	465 ± 198	6.91 ± 0.25	0.80 ± 0.08	0.46 ± 0.07	4.79 ± 0.26
October 2007	353 ± 119	6.95 ± 0.12	0.77 ± 0.07	0.42 ± 0.06	5.01 ± 0.47
April 2008	136 ± 72	7.09 ± 0.08	0.77 ± 0.07	0.40 ± 0.06	ND
July 2008	290 ± 185	7.03 ± 0.14	0.80 ± 0.25	0.58 ± 0.31	ND
October 2008	528 ± 540	6.89 ± 0.13	0.79 ± 0.12	0.41 ± 0.09	4.92 ± 0.32
Average	354 ± 304	6.97 ± 0.17	0.79 ± 0.13	0.45 ± 0.16	4.90 ± 0.36
Rank	A	C	B	B	A
F	23.90	201.80	23.90	165.90	21.20
p	0.014	<0.001	0.014	<0.001	0.017

The overall average across all sample dates is given, and rank denotes significant differences between sites (sites that do not share the same letter are significantly different; Tukey post-hoc; $p < 0.05$) based on a repeated measures analysis of variance ($F_{(2,3)}$ statistics and p values are given at bottom)

Table 4 Rates of sulfate reduction, acetoclastic methanogenesis, and hydrogenotrophic methanogenesis on five samples dates at three sites along the salinity gradient in the Delaware River Estuary, U.S. Averages (±SD) for each date are depth integrated (to a depth of 16 cm) in duplicate soil cores ($n = 2$)

Date	Sulfate reduction (mmol SO_4^{2-} m^{-2} d^{-1})	Acetoclastic methanogenesis (mmol CH_4 m^{-2} d^{-1})	Hydrogenotrophic methanogenesis (mmol CH_4 m^{-2} d^{-1})
Tidal fresh			
July 2007	2.72 ± 1.66	8.16 ± 3.53	1.34 ± 0.30
October 2007	8.13 ± 2.77	9.83 ± 5.10	1.24 ± 0.20
April 2008	8.99 ± 1.22	2.87 ± 1.73	0.08 ± 0.11
July 2008	0.87 ± 0.56	21.97 ± 10.76	0.40 ± 0.39
October 2008	4.97 ± 6.48	1.79 ± 2.09	1.17 ± 1.66
Average	5.14 ± 4.08	8.92 ± 8.69	0.85 ± 0.79
Rank	A	B	
Oligohaline			
July 2007	10.71 ± 10.57	1.11 ± 0.17	0.34 ± 0.07
October 2007	28.78 ± 9.36	2.65 ± 0.20	0.03 ± 0.04
April 2008	0.59 ± 0.58	3.18 ± 1.80	0.00 ± 0.00
July 2008	4.34 ± 0.52	8.82 ± 2.88	1.85 ± 2.60
October 2008	9.51 ± 2.61	0.37 ± 0.38	0.59 ± 0.04
Average	10.79 ± 11.30	3.23 ± 3.34	0.56 ± 1.12
Rank	A	A	
Mesohaline			
July 2007	34.18 ± 9.41	0.41 ± 0.09	0.06 ± 0.05
October 2007	16.86 ± 7.82	0.29 ± 0.13	0.00 ± 0.00
April 2008	14.50 ± 4.35	0.31 ± 0.01	0.00 ± 0.00
July 2008	50.71 ± 11.23	2.01 ± 2.39	0.00 ± 0.00
October 2008	7.75 ± 2.33	1.82 ± 2.52	0.00 ± 0.00
Average	24.80 ± 17.44	0.97 ± 1.42	0.01 ± 0.03
Rank	B	A	
F	30.05	45.50	3.56
p	0.010	0.006	0.161

The overall average across all sample dates ($n = 10$) is given, and rank denotes significant differences between site averages (sites that do not share the same letter are significantly different; Tukey post-hoc; $p < 0.05$) based on repeated measures ANOVA ($F_{(2,3)}$ statistics and p values are given at bottom)

dynamics between 2007 and 2008 at the freshwater site (Fig. 6). During winter months (October–March) there was little NEP, though the tidal freshwater site was a source of C to the atmosphere during the fall and early winter (Fig. 6). On an annual basis, there were marginally significant differences between rates of NEP ($F_{(2,15)} = 3.50$; $p = 0.057$). The mesohaline marsh was net carbon sink in both years, as was the tidal freshwater marsh site in 2007 (Fig. 7). The oligohaline marsh was a net carbon source to the atmosphere in 2007, and both the tidal freshwater and oligohaline sites were carbon neutral in 2008 (Fig. 7). Due to the high ER_{CH_4} at the oligohaline site during

summer months (Fig. 6), this site was a large source of GHG to the atmosphere peaking at over 800 g $CO_{2\text{-eq}}$ m^{-2} $month^{-1}$ released in both summers (Fig. 6), and on an annual basis this marsh was a source of over 2000 g $CO_{2\text{-eq}}$ m^{-2} $year^{-1}$ to the atmosphere (Fig. 7). The tidal freshwater site was a GHG sink in 2007 linked to the large uptake of C through GEP and modest ER_{CH_4}, but was a GHG source in 2008 due to more modest GEP coupled with the release of CH_4 (Fig. 7). The salt marsh site was consistently a sink for GHG, with highest rates of GHG sequestration in summer months (Fig. 6). Annually, the salt marsh sequestered 550–700 g $CO_{2\text{-eq}}$ m^{-2} $year^{-1}$ (Fig. 7).

Table 5 Coefficients and intercepts for linear regressions of porewater biogeochemical inventories and rates of microbial processes against porewater chloride (Cl^-) inventories and temperature (if coefficients for both Cl^- and temperature are given, these independent variables were both significant predictors in a multiple regression) for data across all three sites combined (tidal freshwater, oligohaline, and mesohaline) along the salinity gradient in the Delaware River Estuary

	Coefficients			R^2	p
	Chloride inventory (mol Cl^- m^{-2})	Temperature (°C)	Intercept		
Porewater inventories (mmol m^{-2})					
DIC	14.99		71.0	0.39	<0.001
PO_4^{3-}	0.45	−0.34	14.5	0.27	0.014
H_2S	2.38		−4.0	0.53	<0.001
DOC		15.25	56.8	0.28	0.003
Acetate	−1.04	0.96	8.6	0.24	0.025
Total LMW-OAs	−3.72	3.43	75.0	0.36	0.003
Microbial rates (mmol m^{-2} d^{-1})					
Sulfate reduction	1.14	0.39	−2.6	0.50	<0.001
Hydrogenotrophic methanogenesis	−0.04	0.03	0.4	0.20	0.046
Acetoclastic methanogenesis	−0.37	0.35	1.3	0.42	0.001

The R^2 and p values of the regressions are given

Modeled annual rates of ER_{SR} increased from 30 g C m^{-2} $year^{-1}$ in the tidal freshwater marsh to about 170 g C m^{-2} $year^{-1}$ in the salt marsh (Fig. 8). ER_{MG} decreased from about 50 g C m^{-2} $year^{-1}$ in the freshwater marsh to 10 g C m^{-2} $year^{-1}$ in the salt marsh. Intermediate rates of ER_{SR} and ER_{MG} were modeled at the oligohaline site (Fig. 8). The contribution of ER_{SR} to total ER (f_{SR}) was about 4 % in the tidal freshwater soils, with methanogenesis (f_{MG}) contributing between 5 and 8 % (Fig. 8). f_{SR} increased at the oligohaline site to around 10 %, and f_{MG} dropped to 5 %. At the mesohaline site, f_{SR} increased to 30–45 %, while f_{MG} declined to about 2 % (Fig. 8). The estimated contribution of plant respiration to ER (f_{Plant}) was 35–60 % (Fig. 8)

Long term carbon accretion rates

Rates of accretion based on ^{210}Pb and ^{137}Cs radiodating ranged from 0.17 to 1.65 cm $year^{-1}$ (Table 6). ^{137}Cs dating indicated lower rates of accretion than ^{210}Pb dating. Accretion at the tidal freshwater site was substantially lower than at the other sites (Table 6). The ^{210}Pb data for the tidal freshwater marsh indicated a shift in accretion rates between more recently deposited soils (0.25 cm $year^{-1}$ in top 8 cm of profile) and deeper soils (15.7 cm $year^{-1}$ in remainder of profile; data not shown). When coupled with soil organic C content (Table 3), rates of calculated C accretion ranged from 75 to 336 g C m^{-2} $year^{-1}$ (Table 3). Because of significantly lower soil density and organic C content at the oligohaline site (Table 3), rates of C accretion at this site were lower than at the salt marsh. Modeled rates of NEP were 35–70 % of measured long term accretion rates at the mesohaline site (Table 6). In contrast, there were substantial differences between NEP and long term accretion at the tidal freshwater and oligohaline sites (Table 6).

Discussion

Marsh productivity

Tidal marshes along the salinity gradient in the Delaware River Estuary are productive wetlands, with annual aboveground biomass production exceeding 400 gdw m^{-2} (Table 2; Fig. 3). These rates of productivity generally agree with those from previous studies (Smith et al. 1979; Schubauer and Hopkinson 1984; Doumelele 1981; Whigham et al. 1978; Neubauer et al. 2000). Annual aboveground biomass production in *S. alterniflora* salt marshes generally ranges from 400 to over 3,000 gdw m^{-2} $year^{-1}$, though the higher rates are generally for tall-form *S.*
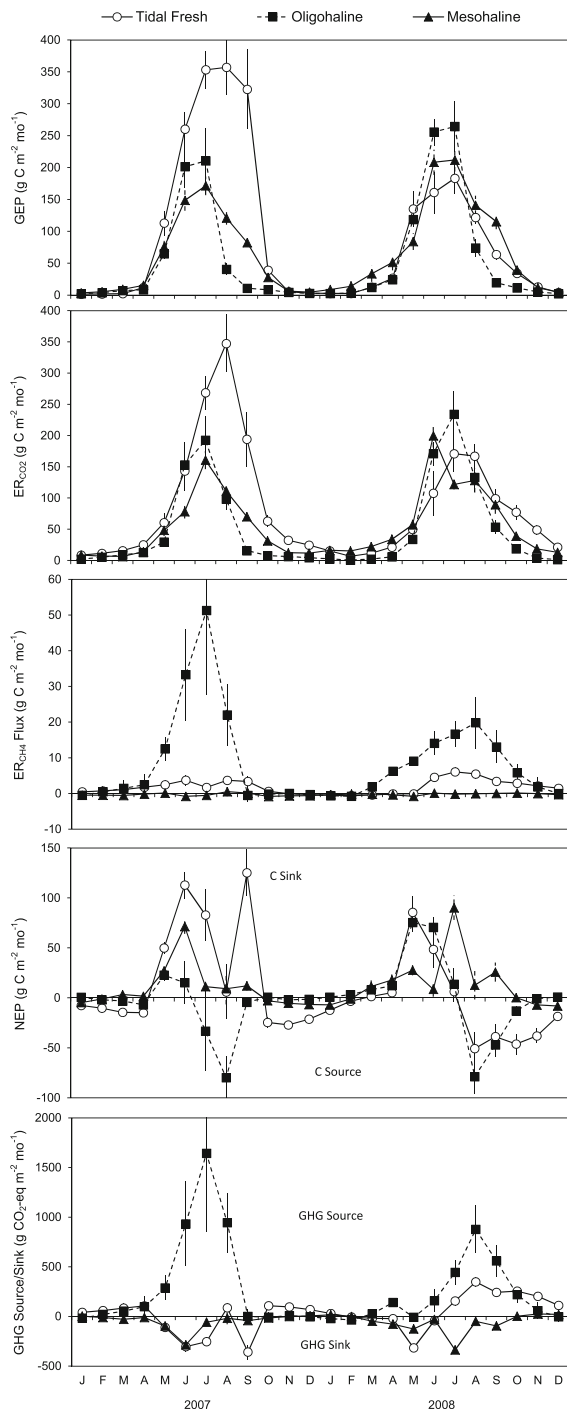
Fig. 6 Monthly rates of gross ecosystem production (GEP), ecosystem respiration to CO_2 (ER_{CO_2}) and CH_4 (ER_{CH_4}), net ecosystem production (NEP), and greenhouse gas (GHG) source or sink status for three sites over 2 years from the carbon exchange model
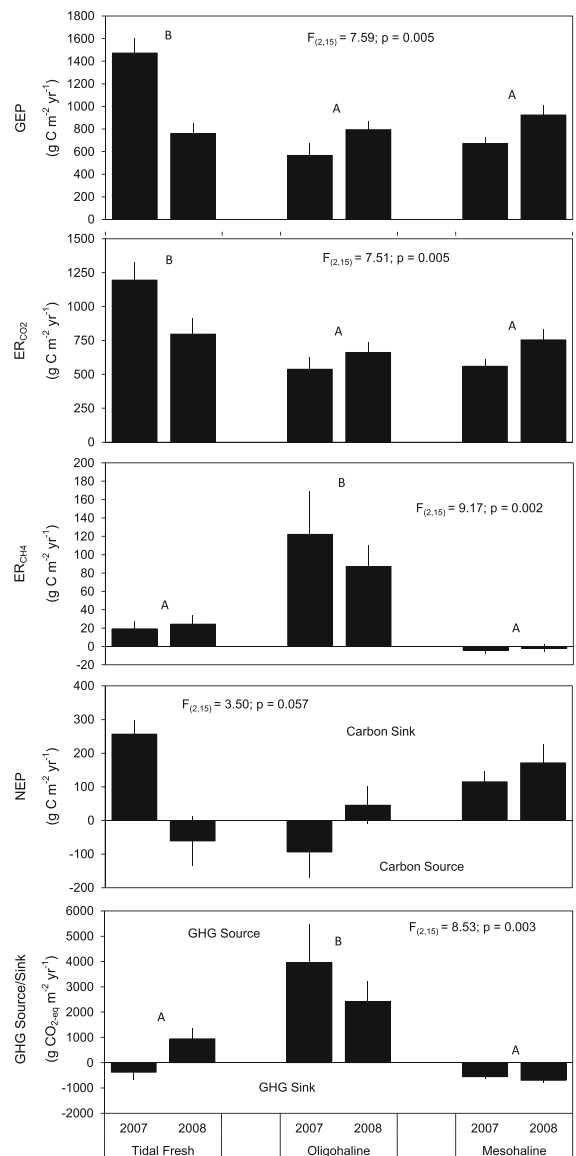
Fig. 7 Annual rates of gross ecosystem production (GEP), ecosystem respiration to CO_2 (ER_{CO_2}) and CH_4 (ER_{CH_4}), net ecosystem production (NEP), and greenhouse gas (GHG) source or sink at three sites over two years from the carbon exchange model. Rates within a panel that do not share a letter are significantly different (rmANOVA with Tukey post hoc; $p < 0.05$)

alterniflora in lower latitude marshes (Schubauer and Hopkinson 1984). For instance, Smith et al. (1979) measured 500 gdw m^{-2} year^{-1} of short-form *S. alterniflora* aboveground production in a New Jersey salt marsh, similar to production measured at the mesoh-

Fig. 8 Annual rates of ecosystem respiration via sulfate reduction (ER$_{SR}$) and acetoclastic methanogenesis (ER$_{MG}$) from the carbon exchange model, and the contribution of plant respiration (f$_{Plant}$), sulfate reduction (f$_{SR}$) and methanogensis (f$_{MG}$) to total ecosystem respiration. The bars represent the range in f$_{Plant}$ derived assuming plants respire between 40 and 50 % of the C they fix through GEP
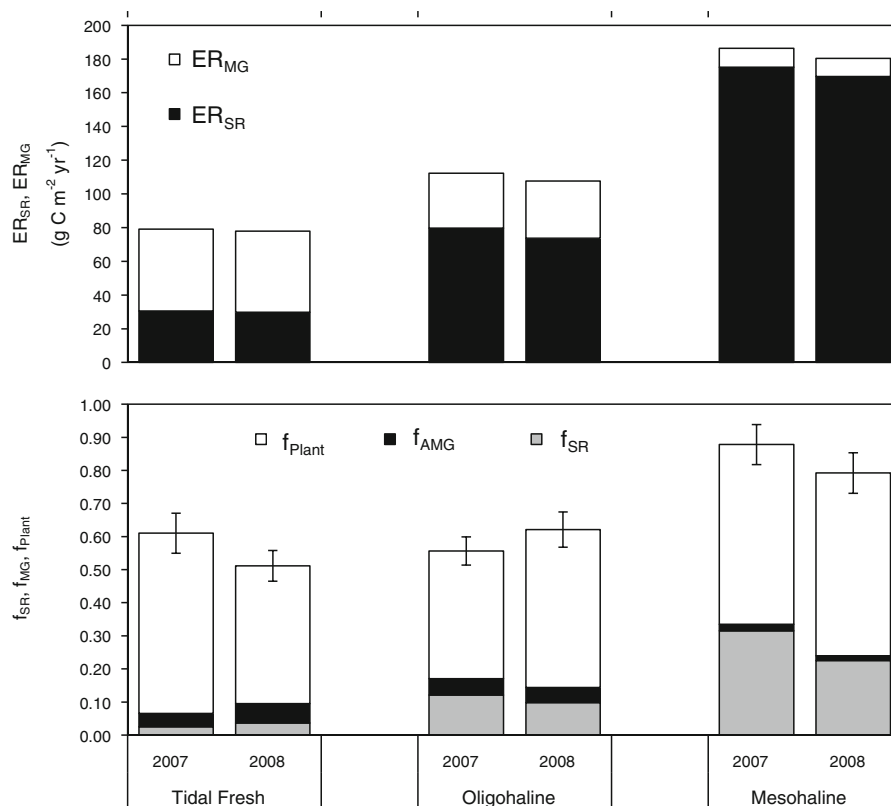
Table 6 Rates of marsh accretion measured by ^{210}Pb and ^{137}Cs radiodating, calculated C accumulation rates using these accretion rates and soil organic C content from each site (Table 3), and modeled net ecosystem productivity (NEP) for two years (Fig. 7)

	Tidal Fresh	Oligohaline	Mesohaline
Measured accretion rate (cm year^{-1})			
^{210}Pb	0.25	1.65	1.51
^{137}Cs	0.17	1.46	1.15
Calculated C accretion rate (g C m^{-2} year^{-1})			
^{210}Pb	109.8	250.4	335.8
^{137}Cs	75.4	220.8	256.6
Modeled NEP (g C m^{-2} year^{-1})			
2007	256.9	−93.5	115.3
2008	−60.7	45.4	171.4

aline salt marsh (Fig. 3; Table 2). Fewer data exist for biomass production in freshwater marshes, but reported annual aboveground production in *P. virginica* dominated marshes range from 600 to 900 gdw m^{-2} year^{-1} (Doumelele 1981; Whigham et al. 1978; Neubauer et al. 2000). Aboveground

biomass production at the tidal freshwater site ranged from 360 to 1,550 gdw m^{-2} year^{-1} (Table 2), indicating tidal freshwater marshes can be as or more productive than salt marshes in the Delaware River Estuary, and that tidal freshwater marshes exhibit substantial interannual variability in productivity. A mixed community of annual plants dominated by *Bidens* but also including *Z. aquatica*, *A. rudis*, and *Polygonum* species grew at the tidal freshwater site and contributed to the very high aboveground biomass and photosynthetic efficiency in 2007, but not in 2008 or 2009 for reasons that are not clear (Fig. 3). In contrast, the *P. virginica* biomass was relatively constant over these same three years (Fig. 3). The large interannual variability in aboveground biomass resulted in no clear pattern of productivity along the salinity gradient (Table 2).

Plants translocate C, N, and other materials between roots and aboveground biomass, and translocation in perennial plants such as *S. alterniflora* and *P. virginica* from belowground reserves can support substantial aboveground biomass accumulation early in the growing season in both tidal freshwater marshes

(Neubauer et al. 2000) and salt marshes (Hopkinson and Schubauer 1984; Dai and Wiegert 1996). Prior to senescence in the fall, plants translocate C and N from aboveground biomass to belowground roots and rhizomes (Hopkinson and Schubauer 1984; Dai and Wiegert 1996; Neubauer et al. 2000). Belowground biomass, not measured in this study, can exceed aboveground biomass for many tidal freshwater and salt marsh plants (Whigham 1978; Schubauer and Hopkinson 1984). Because of bi-directional translocation at different times of year, the difficulty in measuring belowground production, and uncertainties in rates of aboveground and belowground tissue turnover rates, determining total plant (above- and belowground) productivity using biomass harvests is difficult and prone to error (Dai and Wiegert 1996; Neubauer et al. 2000). The gas flux method employed in this study can provide a more accurate measurement of total production by integrating above- and below-ground processes (Neubauer et al. 2000).

Annual GEP from the gas flux model, which accounts for both above- and below-ground production, ranged from 560 to 1,470 g C m^{-2} $year^{-1}$ (Fig. 7). These data generally agree with published rates of marsh productivity. For instance, Dai and Wiegert (1996) found short-form *S. alterniflora* productivity of 749 g C m^{-2} $year^{-1}$ in a Georgia salt marsh. Neubauer et al. (2000) measured annual gross macrophyte photosynthesis rates of 1,000 g C m^{-2} $year^{-1}$ in a *P. virginica* dominated tidal freshwater marsh in Virginia. In the Delaware River Estuary, GEP was significantly correlated with peak aboveground biomass C [GEP (g C m^{-2} $year^{-1}$) = 1.53 × Biomass (g C m^{-2}) + 402; R^2 = 0.63; $p <$ 0.001; data from all sites in both years], and aboveground biomass accounted for 10–60 % of the C fixed via photosynthesis. Belowground biomass production, plant respiration, herbivory, export of dissolved and particulate organic C in estuarine waters, and heterotrophic decomposition in marsh soils account for the remaining C (Dai and Wiegert 1996; Neubauer et al. 2000).

We observed high interannual variability in biomass production at all of the study sites, though most notably at the tidal freshwater site (Table 2). In the absence of competition, *S. alterniflora* grows most vigorously and produces the most biomass in freshwater conditions (Phleger 1971; Webb 1983). Interannual variability in salt marsh productivity has been attributed to variations in summer soil porewater salinities driven by variations in sea-level and rainfall (Morris and Haskin 1990). The three years of biomass data at the oligohaline and mesohaline sites demonstrate clear negative relationships between peak aboveground biomass and the average salinity over the prior month (Fig. 4). Relatively small precipitation events in the mid- and late-summer, as occurred repeatedly in 2009 but not in the preceding two years, are sufficient to increase river discharge and lower estuarine salinities (Fig. 2), stimulating greater biomass production (Fig. 4).

The interannual variability at the tidal freshwater marsh site may be due to inconsistent recruitment of annuals from the seed-bank and/or subsequent establishment and persistence of the annuals over the growing season (Leck and Simpson 1995). The perennial *P. virginica* demonstrated relatively constant biomass over the three years, while the annuals (dominated by *Bidens* and *Polygonum* species) produced substantial biomass in 2007 but not in 2008 and 2009 (Fig. 3). Leck and Simpson (1995) observed high interannual variability in the seed bank, seedling density, and mature vegetation cover in a Delaware River tidal freshwater marsh over a 10 year study, and species varied independently in an unpredictable manner. Relatively small changes in flooding (<10 cm) early in the growing season during plant germination can significantly alter recruitment from the seed-bank and subsequent species composition and densities (Baldwin et al. 2001). Early season (mid-May to mid-June) discharge from the Delaware River was lower in 2007 than other years and well below the long-term average (Fig. 2). Lower river discharge may have resulted in less flooding of the marsh surface in the upper tidal freshwater region and promoted vigorous recruitment and establishment of the freshwater plant community in 2007 (Fig. 3).

Despite substantial aboveground biomass production at the oligohaline site (Fig. 3), annual NEP suggests this marsh is not accumulating C (Figs. 6, 7). The marsh is a net CO_2 sink in the spring as biomass accumulates, but then loses both CO_2 and CH_4 to the atmosphere in the late summer and early fall of both years (Fig. 6). This C loss corresponds to the early decline of *Z. aquatica* aboveground biomass and low photosynthetic efficiency (Fig. 3), and therefore low GEP (Fig. 6). While ER_{CO_2} and ER_{CH_4} also decline in late summer, likely due to lack of new organic matter

inputs, ER exceeds GEP and the marsh becomes a source of C to the atmosphere (Fig. 6). These data suggest that nearly all of the annual C accumulation in *Z. aquatica* biomass was respired as CO_2 or CH_4.

We hypothesize that the early decline in *Z. aquatica* biomass at the oligohaline site is a consequence of seasonal salt-water intrusion. Decline in *Z. aquatica* biomass in August is not typical of the lifecycle of this plant, which has been shown to senesce in late September (Whigham and Simpson 1977). *Z. aquatica* is a freshwater plant that can tolerate low levels of salt, but conductivities exceeding 8 mS cm^{-1} (equivalent to a salinity of 4.5) were measured at this site in the summers of 2007 and 2008 (Fig. 2). Under experimental conditions, declines in plant production have been observed at similar or lower salinities (Willis and Hester 2004; Spalding and Hester 2007; Neubauer 2013; Sutter et al. 2014). These concentrations of salts are likely to cause plant stress, and may be sufficient to result in plant death as apparently observed at the late summer at the oligohaline site (Fig. 3). Intrusion of salt-water in the late summer at this site is controlled by discharge from the Delaware River, and higher summer discharge kept salinities lower in 2009 than in the previous two years (Fig. 2). Biomass production of *Z. aquatica* was higher in 2009 than in the preceding two years, and there was a negative relationship between salinity (conductivity) and aboveground biomass production at the oligohaline site (Fig. 4).

The *Z. aquatica* community at the oligohaline site likely cannot tolerate multiple years of seasonal saltwater intrusion, and this site may be in a state of transition from an oligohaline marsh to a mesohaline marsh dominated by more salt-tolerant plants (*S. alterniflora* or the invasive *Phragmites australis* which has been observed in nearby locations) or a non-vegetated mudflat if the site does not keep pace with relative sea-level rise. The long-term salinity record (40 yr) indicates that salinity has increased by over 1.0 in this region of the Delaware Estuary irrespective of discharge, due to sea-level rise and dredging of the main channel (Ross 2013). The low salinity conditions observed during 2009 accompanied summer discharge events notably higher than the long-term average (Fig. 2). The seasonal (late summer) salinity intrusion observed in 2007 and 2008 occurred during more normal summer discharge conditions (Fig. 2), suggesting that seasonal salt-water intrusion

of levels lethal to *Z. aquatica* will likely become a more common occurrence.

Microbial respiration and soil biogeochemistry

There were clear patterns of microbial respiration along the estuarine salinity gradient indicating increasing rates of sulfate reduction and decreasing rates of methanogenesis from tidal freshwater to mesohaline marshes (Fig. 8; Table 4). There were significant relationships between porewater Cl$^-$ and rates of methanogenesis (negative) and sulfate reduction (positive; Table 5). As would be expected by the greater availability of SO_4^{2-} in salt marsh soils and the greater thermodynamic yield of sulfate reduction compared to methanogenesis (Capone and Kiene 1988), rates of sulfate reduction were higher in the mesohaline salt marsh (Fig. 8; Table 4). Conversely, the relative lack of SO_4^{2-} at the tidal freshwater site resulted in higher rates of methanogenesis (Fig. 8; Table 4). Rates of all microbial processes increased with temperature (Table 5) due to the temperature sensitivity of the microbial communities and to higher organic matter availability from plant growth during the summer (Hines et al. 1989; Figs. 3, 6). The concentration of labile LMW-OAs (including acetate) that are typically directly available to anaerobic microbial respiration increased with temperature but decreased with salinity (Table 5), and DOC increased with temperature (Table 5) indicating that plant exudation of labile dissolved carbon compounds during the growing season likely fueled a portion of microbial respiration (Hines et al. 1999; Strobel 2001; Oliveira et al. 2010).

The combined contribution of sulfate reduction and methanogenesis to total ER (f_{SR} and f_{MG}, respectively) increased from less than 10 % at the tidal freshwater site to 25–30 % at the salt marsh site (Fig. 8). Plant respiration accounts for around 40–50 % of carbon fixed via photosynthesis in both freshwater marshes (Neubauer et al. 2000) and salt marshes (Dai and Wiegert 1996). At the mesohaline site, then, plant respiration and sulfate reduction together account for more than 80 % the ecosystem respiration (Fig. 8). Due to high concentrations of SO_4^{2-} in saline floodwater in salt marshes and the limited availability of other electron acceptors in anaerobic soils, sulfate reduction can account for up to 100 % of anaerobic decomposition in salt marsh soils (Howarth and Giblin

1983; Howarth 1993), though iron reduction can also account for a large fraction of organic matter mineralization (Gribsholt et al. 2003; Tobias and Neubauer 2009).

Respiration pathways other than sulfate reduction and methanogenesis, or significant sulfate reduction and/or methanogenesis below 20 cm (the greatest depth of measurements), are necessary to account for the 'missing' respiration at the tidal freshwater and oligohaline sites (Fig. 8). Heterotrophic aerobic respiration is likely to account for a portion of the total ER (Tobias and Neubauer 2009). SO_4^{2-}, supplied largely via diffusion from the overlying water, is typically depleted with depth in these marsh soils to concentrations below detection by 10 cm (data not shown). Significant sulfate reduction at depths below 20 cm is therefore unlikely. In contrast, methanogenesis does not require an outside electron acceptor, and measured rates of acetoclastic methanogenesis generally increased with depth at oligohaline and tidal freshwater sites (data not shown). At the tidal freshwater marsh, rates of CH_4 generated by acetoclastic methanogenesis and hydrogenotrophic methanogenesis (approximately 25 g C–CH_4 m^{-2} year^{-1}) were approximately balanced by rates of CH_4 release (22 g C m^{-2} year^{-1}; Fig. 7). Microbial CH_4 oxidation would be expected to consume some portion of the CH_4 produced (Megonigal and Schlesinger 2002), but the balance between consumption and generation suggests that deep methanogenesis would not account for the majority of 'missing' ER in the tidal freshwater marsh. Microbial iron reduction can be an important pathway of organic matter decomposition in tidal wetlands, as iron reducers can outcompete methanogens when plant oxygenation of the rhizosphere supplies oxidized iron substrates (Neubauer et al. 2005). It is therefore likely that microbial iron reduction made significant contributions to total ER at both the tidal freshwater and oligohaline sites. Denitrification may also contribute to total microbial respiration, especially in tidal freshwater marsh soils where watershed-derived nitrogen is first introduced into estuarine systems (Seitzinger 1988; Hopfensperger et al. 2009), although denitrification is probably not a dominant pathway of C mineralization in tidal freshwater or saline marsh soils (Megonigal and Neubauer 2009; Tobias and Neubauer 2009).

Measured fluxes of CH_4 from soils at the oligohaline site (Fig. 3) were surprisingly high (90–120 g C m^{-2} year^{-1}; Fig. 7) and were substantially higher than CH_4 produced from rates of acetoclastic methanogenesis and hydrogenotrophic methanogenesis (about 15 g C m^{-2} year^{-1}; Fig. 8). This suggests that significant amounts of CH_4 were generated by methanogenesis at depths >20 cm in the soil profile in oligohaline marsh soils. The CH_4 flux rates measured at the oligohaline site are among the highest reported for tidal marshes (Bridgham et al. 2006), and it is curious that this site had higher CH_4 fluxes than the tidal freshwater site (Fig. 7). The high CH_4 fluxes at the oligohaline site contribute substantially to total ER. ER_{CH_4} accounts for 10–20 % of total ER in the oligohaline marsh and only 2–3 % in the tidal freshwater marsh. Typically, methanogenesis declines with increasing SO_4^{2-} availability as sulfate reducers outcompete methanogens for organic matter substrates, leading to a gradient in CH_4 fluxes from tidal marshes that mirrors the salinity gradient in estuaries (DeLaune et al. 1983; Bartlett et al. 1987). Poffenbarger et al. (2011) found that oligohaline marshes had higher CH_4 fluxes than either tidal fresh or more saline marshes, which they attribute to depletion of pore-water SO_4^{2-} and methane producing microsites in low salinity soils. However, Weston et al. (2011) observed significant overlap between sulfate reduction and methanogenesis with depth and increased CH_4 emissions following salt-water intrusion into tidal freshwater marsh soils, and CH_4 fluxes were not correlated with porewater SO_4^{2-} concentrations at the oligohaline site in the current study, suggesting mechanisms other than SO_4^{2-} depletion are responsible for the CH_4 emissions from the oligohaline marsh (Figs. 3, 6 and 7).

The plant community plays an important role in influencing rates of microbial organic matter mineralization (Sutton-Grier and Megonigal 2011). Plants supply organic matter substrates that can fuel methanogenesis (Vann and Megonigal 2003), and methanogenesis and CH_4 emissions from wetland soils are largely controlled by rates of plant production (Whiting and Chanton 1993). GEP was higher at the tidal freshwater site than at the oligohaline site in 2007 and similar in 2008 (Fig. 7) indicating different rates of methanogenesis were not linked directly to differences in plant production. Plants can further influence pathways of microbial respiration (Roden and Wetzel 1996) and CH_4 exchange between wetland soils and the atmosphere (Whiting and Chanton 1996) via gas

transport through plant tissue. Wetland plants transport oxygen to roots through either passive diffusion or pressurized convective flow (Dacey 1981; Armstrong and Armstrong 1991; Brix et al. 1992). While biomass and annual production at the two fresher sites were similar, the plant communities were quite different (Fig. 3). There was a mix of perennial and annual plant species in the tidal freshwater marsh, and the perennial *P. virginica* was one of the dominant plants. *P. virginica* has very high belowground biomass, with a belowground: aboveground biomass ratio exceeding 8.0 and rhizomes that can reach depths of 3 m (Whigham et al. 1978). The monoculture of the annual *Z. aquatica* in the olighaline marsh would have significantly lower belowground biomass (with a belowground: aboveground biomass ratio less than 0.5; Whigham et al. 1978) and a root system within the top 30 cm of the soil profile. The high belowground biomass and deep rooting *P. virginica* may therefore supply more oxygen to soils. Oxygen in the rhizosphere can promote methane oxidation (Watson et al. 1997) and oxidize reduced compounds providing a source of electron acceptors such as iron oxides that yield greater energy than methanogenesis when coupled to organic matter oxidation, suppressing CH_4 production and emission at the tidal freshwater site (Neubauer et al. 2005; Sutton-Grier and Megonigal 2011).

Wetland plants can also regulate CH_4 flux by acting as a conduit for CH_4 from soils to the atmosphere (Sebacher et al. 1985; Chanton et al. 1992; Sorrel and Boon 1994; Sutton-Grier and Megonigal 2011). *P. virginica* and *Z. aquatica* both have aerenchymous tissue, and CH_4 fluxes have been shown to be higher from wetland soils with either *P. virginica* (Chanton et al. 1992; Sutton-Grier and Megonigal 2011) or *Zizania latifolia* (Inamori et al. 2007; Wang et al. 2013; *Z. latifolia* is closely related and morphologically similar to *Z. aquatica*) than from unvegetated soils, indicating both plant types facilitate CH_4 production and/or transport. The complex interactions between plant delivery of both electron donors (organic matter) and electron acceptors (oxygen and other subsequently oxidized substrates) and plant-mediated transport of both oxygen and CH_4 that can vary between plant types (pressurized vs. diffusive gas flow, plant rooting depth, and belowground biomass) clearly influence CH_4 production, oxidation, and transport dynamics (Sebacher et al. 1985; Brix et al.

1992; Chanton et al. 1992; Sorrel and Boon 1994; Sutton-Grier and Megonigal 2011), but our understanding of these interactions is currently limited (i.e., Keller et al. 2013). Mechanisms for high CH_4 emissions at the oligohaline site are therefore not clear, though we suspect that saltwater intrusion may play a role.

As with the plant community, the microbial community and soil biogeochemical processes are likely in transition at the oligohaline site due to saltwater intrusion. The intrusion of salt-water has been shown to enhance microbial sulfate reduction and methanogenesis, possibly due to changes in organic matter lability in freshwater soils upon the introduction of salts (Weston et al. 2011). Contrary to predictions based on thermodynamic energy yields, the introduction of salt-water may stimulate both sulfate reduction and methanogenesis and promote overall organic matter decomposition (Weston et al. 2011). The high rates of ER_{CH_4} at the oligohaline site (Fig. 3) together with the lack of organic matter sequestration (Fig. 7) suggests that salt-water intrusion may be stimulating microbial organic matter decomposition and inhibiting the sequestration of organic matter. This, together with the transition in the plant community discussed above, may limit the ability of this marsh to keep pace with sea-level rise and promote the transition into an unvegetated mudflat.

Ecosystem gas exchange and C sequestration

The rates of NEP reported here represent only gas exchange between the marsh and the atmosphere, and do not account for deposition of C associated with sediments on the marsh surface or export of C from the marsh in particulate or dissolved forms (Odum and Heywood 1978). The rates given here should therefore not be taken for absolute rates of C sequestration, as they may over- or under-estimate actual rates due to deposition and export of C. The C exchange model describes C cycling at three sites along the salinity gradient in 2007 and 2008, with relatively low summer discharge and therefore high conductivities at the oligohaline and mesohaline sites (Fig. 2). Unfortunately the sampling frequency was not sufficient to allow modeling of ecosystem C cycling in a lower salinity year (such as 2009). Additionally, we did not quantify nitrous oxide (N_2O) exchange rates between marsh soils and the atmosphere, which may alter the

GHG balances reported here because of the large warming potential of N_2O (Forster et al. 2007). Tidal wetlands can be a source of N_2O to the atmosphere (Adams et al. 2012; Tong et al. 2013; Sun et al. 2014). The contribution of N_2O to total GHG emissions from saline marshes is typically low (Hirota et al. 2007; Livesley and Andrusiak 2012), though N_2O emissions may be higher from freshwater marshes (Smith et al. 1983) or marshes receiving watershed N inputs (Moseman-Valtiera 2012). A complete GHG balance would require an understanding of N_2O exchange along the estuarine salinity gradient, though N_2O emissions are not likely to significantly alter the GHG balance of these wetlands (Moseman-Valtiera 2012).

At the mesohaline salt marsh site, GEP exceeds ER and there is little CH_4 release (Fig. 7). This salt marsh is therefore consistently a C and GHG sink (Figs. 6 and 7), sequestering 100–340 g C m^{-2} $year^{-1}$ as determined by both the gas exchange model and long-term C accumulation measurements (Table 6). This is similar to the global average rate of C sequestration (210 g C m^{-2} $year^{-1}$) found in a data compilation by Chmura et al. (2003). Salt marshes are productive wetland ecosystems that sequester C in soils with little CH_4 emission due to the high availability of alternate electron acceptors, and have been recognized as important zones for C sequestration (Chmura et al. 2003; Mcleod et al. 2011; Andrews et al. 2012; Chmura 2013).

Tidal freshwater wetlands, though accounting for a modest proportion of total wetland area in most coastal systems, are very productive ecosystems that have received growing but still relatively little attention from the scientific community (Neubauer et al. 2000; Barendregt et al. 2009). While freshwater wetlands can sequester significant quantities of C, the short-term benefits of this C sequestration may be largely counterbalanced by fluxes of CH_4 from freshwater wetland soils. In the Delaware River, the tidal freshwater marsh was a C sink in 2007 but C neutral in 2008, and sequestration of C was largely offset by modest emissions of CH_4 (Fig. 7). There appears to be large inter-annual variability in GEP and ER in this freshwater site, leading to substantial differences in year-to-year C sequestration and GHG exchange rates (Fig. 7). Long-term C accumulation measurements indicate that C sequestration is more modest in this tidal freshwater marsh (about 100 g C m^{-2} $year^{-1}$; Table 6) than at the saltwater site. Despite higher soil

organic C content of tidal freshwater soils (Table 3), the rate of recent vertical accretion at the tidal freshwater site was substantially lower (Table 6). Higher past rates of accretion at this site (15.7 cm $year^{-1}$ based on ^{210}Pb dating; data not shown) suggest that the geomorphology of this tidal freshwater marsh has changed substantially over the past century, likely affecting rates of C sequestration.

The oligohaline marsh appears to be in a state of transition, from a tidal freshwater marsh that sequesters over 200 g C m^{-2} $year^{-1}$ (long-term C accretion estimates; Table 6) to a site that has no net C accumulation (Fig. 7). Saltwater intrusion at this site depresses tidal freshwater plant production in late summer (Fig. 3), and apparently stimulates organic matter decomposition, notably via methanogenesis (Fig. 7). The loss of organic matter via CO_2 and CH_4 turns this site into a relatively large GHG source to the atmosphere (Fig. 7), confirming a previous study of the impacts of salt-water intrusion into freshwater marsh soils on C cycling in the Delaware River Estuary (Weston et al. 2011). Neubauer (2013), however, did not find elevated CH_4 fluxes in response to salt-water intrusion in a South Carolina marsh, suggesting this may be a system-specific response. Future salt-water intrusion may be expected in many tidal freshwater systems as sea-level rise accelerates (Rahmstorf 2007; Milne et al. 2009) and increased evapotranspiration and human water demand result in reduced freshwater inflows (Meehl et al. 2007). Increased organic matter mineralization and reduced plant production will result in little C accumulation, making it difficult for tidal freshwater marshes to keep pace with sea-level rise unless they transition to salt marshes (Weston et al. 2011). Further, salt-water intrusion may produce a minor feedback to climate change through increased GHG emissions. The site-specific response of tidal freshwater marshes to salt-water intrusion warrants further investigation.

Conclusions

Several years of monitoring tidal marshes along the salinity gradient in the Delaware River demonstrated that tidal freshwater, oligohaline, and mesohaline marshes are productive ecosystems. The salt marsh was a consistent sink for atmospheric C and greenhouse gases (GHGs). In contrast, the tidal freshwater

marsh was (depending on the year) either a C sink or C neutral and, because of modest CH_4 emissions, was GHG neutral or a source of GHGs to the atmosphere. Large inter-annual variations in plant productivity drove these patterns in C cycling. Seasonal salt-water intrusion into the oligohaline marsh depressed plant production in the late summer and accelerated organic matter mineralization and CH_4 emissions. Marshes experiencing salt-water intrusion in the Delaware River therefore appear to be a large but likely localized source of GHGs to the atmosphere. The loss of soil organic matter together with the salt-stress on the freshwater plant community will limit vertical accretion potential in tidal freshwater marshes experiencing salt-water intrusion.

References

Adams CA, Andrews JE, Jickells T (2012) Nitrous oxide and methane fluxes vs. carbon, nitrogen and phosphorus burial in new intertidal and saltmarsh sediments. Sci Total Environ 434:240–251

Albert DB, Martens CS (1997) Determination of low-molecular-weight organic acid concentrations in seawater and pore-water samples via HPLC. Mar Chem 56(1–2):27–37

Andrews JE, Jickells TD, Adams CA, Parkes DJ, Kelly SD (2012) Sediment record and storage of organic carbon and the nutrient elements (N, P, Si) in estuaries and near-coastal seas. In: Wolanski E, McLusky D (eds) Treatise on estuarine and coastal science, vol 4. Academic Press, London, pp 9–38

Armstrong J, Armstrong W (1991) A convective through-flow of gases in *Phragmites australis* (Cav.) Trin. ex Steud. Aquat Bot 39:75–88

Baldwin AH, Egnotovich MS, Clarke E (2001) Hydrologic change and vegetation of tidal freshwater marshes: field,

greenhouse, and seed-bank experiments. Wetlands 21(4):519–531

Barendregt A, Whigham D, Baldwin A (2009) Tidal freshwater wetlands. Backhuys, Leiden

Bartlett KB, Bartlett DS, Harriss RC, Sebacher DI (1987) Methane emissions along a salt-marsh salinity gradient. Biogeochemistry 4(3):183–202

Bridgham SD, Megonigal JP, Keller JK, Bliss NB, Trettin C (2006) The carbon balance of North American wetlands. Wetlands 26(4):889–916

Brix H, Sorrell BK, Orr PT (1992) Internal pressurization and convective gas flow in some emergent freshwater macrophytes. Limnol Oceanogr 37:1420–1433

Capone DG, Kiene RP (1988) Comparison of microbial dynamics in marine and fresh-water sediments: contrasts in anaerobic carbon catabolism. Limnol Oceanogr 33(4):725–749

Chambers LG, Osborne TZ, Reddy KR (2013) Effect of salinity-altering pulsing events on soil organic carbon loss along an intertidal wetland gradient: a laboratory experiment. Biogeochemistry 115:363–383

Chanton JP, Whiting GJ, Showers WJ, Crill PM (1992) Methane flux from *Peltandra virginica*: stable isotope tracing and chamber effects. Glob Biogeochem Cycles 6:15–31

Chmura GL (2013) What do we need to assess the sustainability of the tidal salt marsh carbon sink? Ocean Coast Manag 83:25–31

Chmura GL, Anisfeld SC, Cahoon DR, Lynch JC (2003) Global carbon sequestration in tidal, saline wetland soils. Glob Biogeochem Cycles 17(4):1111. doi:10.1029/2002GB001917

Cline JD (1969) Spectrophotometric determination of hydrogen sulfide in natural waters. Limnol Oceanogr 14:454–458

Craft CB, Richardson CJ (1998) Recent and long-term organic soil accretion and nutrient accumulation in the everglades. Soil Sci Soc Am J 62(3):834–843

Dacey JWH (1981) How aquatic plants ventilate. Oceanus 24:43–51

Dai T, Wiegert RG (1996) Estimation of the primary productivity of *Spartina alterniflora* using a canopy model. Ecography 19(4):410–423

Deegan LA, Johnson DS, Warren RS, Peterson BJ, Fleeger JW, Fagherazzi S, Wollheim WM (2012) Coastal eutrophication as a driver of salt marsh loss. Nature 490(7420):388–392

Delaune RD, Smith CJ, Patrick WH (1983) Methane release from Gulf-Coast wetlands. Tellus Ser B Chem Phys Meteorol 35(1):8–15

Doumelele DG (1981) Primary production and seasonal aspects of emergent plants in a tidal fresh-water marsh. Estuaries 4(2):139–142

Forster P, Ramaswamy V, Artaxo P, Berntsen T, Betts R, Fahey DW, Haywood J, Lean J, Lowe DC, Myhre G, Nganga J, Prinn R, Raga G, Schulz M, Van Dorland R (2007) Changes in atmospheric constituents and in radiative forcing. In: Solomon S, Qin D, Manning M, Chen Z, Marquis M, Averyt KB, Tignor M, Miller HL (eds) Climate change 2007: the physical science basis. Contribution of working group I to the fourth assessment report of the intergovernmental panel on climate change. Cambridge University Press, Cambridge

Gribsholt B, Kostka JE, Kristensen E (2003) Impact of fiddler crabs and plant roots on sediment biogeochemistry in a Georgia saltmarsh. Mar Ecol Prog Ser 259:237–251

Hines ME, Knollmeyer SL, Tugel JB (1989) Sulfate reduction and other sedimentary biogeochemistry in a northern New-England salt-marsh. Limnol Oceanogr 34(3):578–590

Hines ME, Evans RS, Genthner BRS, Willis SG, Friedman S, Rooney-Varga JN, Devereux R (1999) Molecular phylogenetic and biogeochemical studies of sulfate-reducing bacteria in the rhizosphere of *Spartina alterniflora*. Appl Environ Microbiol 65(5):2209–2216

Hirota M, Senga Y, Seike Y, Nohara S, Kunii H (2007) Fluxes of carbon dioxide, methane, and nitrous oxide in two contrastive fringing zones of a coastal lagoon, Lake Nakaumi, Japan. Chemosphere 68:597–603

Hopfensperger KN, Kaushal SS, Findlay SEG, Cornwell JC (2009) Influence of plant communities on denitrification in a tidal freshwater marsh of the Potomac River, United States. J Environ Qual 38(2):618–626

Hopkinson CS, Schubauer JP (1984) Static and dynamic aspects of nitrogen cycling in the salt-marsh graminoid *Spartina-alterniflora*. Ecology 65(3):961–969

Howarth RW (1993) Microbial processes in salt-marsh sediments. In: Ford TE (ed) Aquatic microbiology: an ecological approach. Blackwell, Oxford, pp 239–259

Howarth RW, Giblin A (1983) Sulfate reduction in the salt marshes at Sapelo Island, Georgia. Limnol Oceanogr 28(1):70–82

Inamori R, Gui P, Dass P, Matsumura M, Xu K-Q, Kondo T, Ebie Y, Inamori Y (2007) Investigating CH_4 and N_2O emissions from eco-engineering wastewater treatment processes using constructed wetland microcosms. Process Biochem 42:363–373

IPCC (2014) 2013 Supplement to the 2006 IPCC Guidelines for National Greenhouse Gas Inventories: Wetlands. In: Hiraishi T, Krug T, Tanabe K, Srivastava N, Baasansuren J, Fukuda M, Troxler TG (eds) Intergovernmental Panel on Climate Change, Geneva

Jørgensen BB (1982) Mineralization of organic-matter in the sea bed: the role of sulfate reduction. Nature 296(5858):643–645

Kallmeyer J, Ferdelman TG, Weber A, Fossing H, Jørgensen BB (2004) A cold chromium distillation procedure for radiolabeled sulfide applied to sulfate reduction measurements. Limnol Oceanogr 2:171–180

Keller JK, Sutton-Grier AE, Bullock AL, Megonigal JP (2013) Anaerobic metabolism in tidal freshwater wetlands: I. Plant removal effects on iron reduction and methanogenesis. Estuar Coasts 36:457–470

Kirwan ML, Megonigal JP (2013) Tidal wetland stability in the face of human impacts and sea-level rise. Nature 504:53–60

Krauss KW, Whitbeck JL, Howard RJ (2012) On the relative roles of hydrology, salinity, temperature, and root productivity in controlling soil respiration from coastal swamps (freshwater). Plant Soil 358:265–274

Leck MA, Simpson RL (1995) Ten-year seed bank and vegetation dynamics of a tidal freshwater marsh. Am J Bot 82(12):1547–1557

Livesley SJ, Andrusiak SM (2012) Temperate mangrove and salt marsh sediments are a small methane and nitrous oxide source but important carbon store. Estuar Coast Shelf Sci 97:19–27

McKee KL, Mendelssohn IA (1989) Response of freshwater marsh plant community to increased salinity and increased water level. Aquat Bot 34:301–316

McLeod E, Chmura GL, Bouillon S, Salm R, Bjork M, Duarte CM, Lovelock CE, Schlesinger WH, Silliman BR (2011) A blueprint for blue carbon: toward an improved understanding of the role of vegetated coastal habitats in sequestering CO_2. Front Ecol Environ 9(10):552–560

Meehl GA, Stocker TF, Collins WD, Friedlingstein P, Gaye AT, Gregory JM, Kitoh A, Knutti R, Murphy JM, Noda A, Raper SCB, Watterson IG, Weaver AJ, Zhao ZC (2007) Global climate projections. In: Solomon S, Qin D, Manning M, Chen Z, Marquis M, Averyt KB, Tignor M, Miller HL (eds) Climate change 2007: the physical science basis. Contribution of working group I to the fourth assessment report of the intergovernmental panel on climate change. Cambridge University Press, Cambridge

Megonigal JP, Neubauer SC (2009) Biogeochemistry of tidal freshwater wetlands. In: Perillo GME, Wolanski E, Cahoon DR, Brinson MM (eds) Coastal wetlands: An integrated ecosystem approach. Elsevier, Amsterdam, pp 535–562

Megonigal JP, Schlesinger WH (2002) Methane-limited methanotrophy in tidal freshwater swamps. Glob Biogeochem Cycles 16(4):1088. doi:10.1029/2001GB001594

Milly PCD, Dunne KA, Vecchia AV (2005) Global pattern of trends in streamflow and water availability in a changing climate. Nature 438:347–350

Milne GA, Gehrels WR, Hughes CW, Tamisiea ME (2009) Identifying the causes of sea-level rise. Nat Geosci 2:471–478

Mitsch WJ, Bernal B, Nahlik AM, Mander Ü, Zhang L, Anderson CJ, Jørgensen SE, Brix H (2013) Wetlands, carbon, and climate change. Landsc Ecol 28:583–597

Morris JT, Haskin B (1990) A 5-year record of aerial primary production and stand characteristics of *Spartina-alterniflora*. Ecology 71(6):2209–2217

Moseman-Valtierra S (2012) Reconsidering climatic roles of marshes: are they sinks or sources of greenhouse gases? In: Abreu DC, Borbón SL (eds) Marshes: ecology, management and conservation. Nova Science Publishers, Hauppauge, pp 1–48

Murphy J, Riley JP (1962) A modified single solution method for determination of phosphate in natural waters. Anal Chim Acta 26(1):31–36

Neubauer SC (2013) Ecosystem responses of a tidal freshwater marsh experiencing saltwater intrusion and altered hydrology. Estuar Coasts 36(3):491–507

Neubauer SC, Miller WD, Anderson IC (2000) Carbon cycling in a tidal freshwater marsh ecosystem: a carbon gas flux study. Mar Ecol Prog Ser 199:13–30

Neubauer SC, Givler K, Valentine SK, Megonigal JP (2005) Seasonal patterns and plant-mediated controls of subsurface wetland biogeochemistry. Ecology 86(12):3334–3344

Neubauer SC, Franklin RB, Berrier DJ (2013) Saltwater intrusion into tidal freshwater marshes alters the biogeochemical cycling of organic carbon. Biogeosciences 10:8171–8183

Noe GB, Krauss KW, Lockaby BG, Conner WH, Hupp CR (2013) The effect of increasing salinity and forest mortality on soil

nitrogen and phosphorus mineralization in tidal freshwater forested wetlands. Biogeochemistry 114:225–244

Odum WE (1988) Comparative ecology of tidal freshwater and salt marshes. Annu Rev Ecol Syst 19:147–176

Odum WE, Heywood MA (1978) Decomposition of intertidal freshwater plants. In: Good RE, Whigham DF, Simpson RL (eds) Freshwater wetlands, ecological processes and management potential. Academic Press, New York, pp 89–97

Oldfield F, Appleby PG (1984) Empirical testing of ^{210}Pb-dating models for lake sediments. In: Haworth EY, Lund JWG (eds) Lake sediments and environmental history. University of Minnesota, Minneapolis, pp 93–124

Oliveira V, Santos AL, Coelho F, Gomes NCM, Silva H, Almeida A, Cunha A (2010) Effects of monospecific banks of salt marsh vegetation on sediment bacterial communities. Microb Ecol 60(1):167–179

Orcutt B, Boetius A, Elvert M, Samarkin V, Joye SB (2005) Molecular biogeochemistry of sulfate reduction, methanogenesis and the anaerobic oxidation of methane at Gulf of Mexico cold seeps. Geochim Cosmochim Acta 69(17):4267–4281

Pezeshki SR, DeLaune RD, Patrick WH Jr (1987) Response of the freshwater marsh species, Panicum hemitomon Schult., to increased salinity. Freshw Biol 17:195–200

Phleger CF (1971) Effect of salinity on growth of a salt marsh grass. Ecology 52(5):908–911

Poffenbarger HJ, Needelman BA, Megonigal JP (2011) Salinity influence on methane emissions from tidal marshes. Wetlands 31:831–842

Rahmstorf S (2007) A semi-empirical approach to modeling future sea level rise. Science 315:358–360

Redfield AE (1965) Ontogeny of a salt marsh estuary. Science 147:50–55

Ritchie JC, McHenry JR (1990) Application of radioactive fallout cesium-137 for measuring soil-erosion and sediment accumulation rates and patterns: a review. J Environ Qual 19(2):215–233

Roden EE, Wetzel RG (1996) Organic carbon oxidation and suppression of methane production by microbial Fe(III) oxide reduction in vegetated and unvegetated freshwater wetland sediments. Limnol Oceanogr 41:1733–1748

Ross AC (2013) Influences of salinity variability and change in the Delaware Estuary. Thesis, The Pennsylvania State University

Schubauer JP, Hopkinson CS (1984) Above-ground and belowground emergent macrophyte production and turnover in a coastal marsh ecosystem, Georgia. Limnol Oceanogr 29(5):1052–1065

Sebacher DI, Harriss RC, Bartlett KB (1985) Methane emissions to the atmosphere through aquatic plants. J Environ Qual 14:40–46

Seitzinger SP (1988) Denitrification in fresh-water and coastal marine ecosystems: ecological and geochemical significance. Limnol Oceanogr 33(4):702–724

Smith KK, Good RE, Good NF (1979) Production dynamics for above and belowground components of a New-Jersey Spartina-alterniflora tidal marsh. Estuar Coast Mar Sci 9(2):189–201

Smith CJ, DeLaune RD, Patrick WH Jr (1983) Nitrous oxide emission from Gulf Coast wetlands. Geochim Cosmochim Acta 47:1805–1814

Smith SJ, Thomson AM, Rosenberg NJ, Izaurralde RC, Brown RA, Wigley TML (2005) Climate change impacts for the conterminous USA: an integrated assessment: Part 1. Scenarios and context. Climatic Change 69(1):7–25

Solórzano L (1969) Determination of ammonia in natural waters by phenolhypochlorite method. Limnol Oceanogr 14(5):799–801

Sorrel BK, Boon PI (1994) Convective gas-flow in Eleocharis sphacelata R. Br.: methane transport and release from wetlands. Aquat Bot 47:197–212

Spalding EA, Hester MW (2007) Interactive effects of hydrology and salinity on oligohaline plant species productivity: implications of relative sea-level rise. Estuar Coasts 30(2):214–225

Strobel BW (2001) Influence of vegetation on low-molecular-weight carboxylic acids in soil solution: a review. Geoderma 99(3–4):169–198

Sun ZG, Wang LL, Mou XL, Jiang HH, Sun WL (2014) Spatial and temporal variations of nitrous oxide flux between coastal marsh and the atmosphere in the Yellow River estuary of China. Environ Sci Pollut Bull 21:419–433

Sutter LA, Perry JE, Chambers RM (2014) Tidal freshwater marsh plant responses to low level salinity increases. Wetlands 34:167–175

Sutton-Grier AE, Megonigal JP (2011) Plant species traits regulate methane production in freshwater wetland soils. Soil Biol Biochem 43(2):413–420

Syvitski JPM, Kettner AJ, Overeem I, Hutton EWH, Hannon MT, Brakenridge GR, Day J, Vörösmarty C, Saito Y, Giosan L, Nicholls RJ (2009) Sinking deltas due to human activities. Nat Geosci 2(10):681–686

Tobias C, Neubauer SC (2009) Salt marsh biogeochemistry: an overview. In: Perillo GME, Wolanski E, Cahoon DR, Brinson MM (eds) Coastal wetlands: an integrated ecosystem approach. Elsevier, Amsterdam

Tong C, Huang JF, Hu ZQ, Jin YF (2013) Diurnal variations of carbon dioxide, methane, and nitrous oxide vertical fluxes in a subtropical estuarine marsh on neap and spring tide days. Estuar Coasts 36:633–642

Vann CD, Megonigal JP (2003) Elevated CO_2 and water depth regulation of methane emissions: comparison of woody and non-woody wetland plant species. Biogeochemistry 63(2):117–134

Vile MA, Bridgham SD, Wieder RK, Novák M (2003) Response of anaerobic carbon mineralization rates to sulfate amendments in a boreal peatland. Ecol Appl 13:720–734

Wang YH, Ye C, Yang H, Zhang JX, Huang CC, Xie B (2013) Methane formation in soil-plant systems treating wastewater as influenced by microbial populations. Environ Earth Sci 70:1647–1652

Watson A, Stephen KD, Nedwell DB, Arah JRM (1997) Oxidation of methane in peat: kinetics of CH_4 and O_2 removal and the role of plant roots. Soil Biol Biochem 29:1257–1267

Webb JW (1983) Soil-water salinity variations and their effects on Spartina alterniflora. Contrib Mar Sci 26:1–13

Weider RK, Scott KD, Kamminga SK, Vile MA, Vitt DH, Xu B, Benscoter BW, Bhatti JS (2009) Post-fire carbon balance in boreal bogs of Alberta Canada. Glob Change Biol 15:63–81

Weston NB (2014) Declining sediments and rising seas: an unfortunate convergence for tidal wetlands. Estuar Coasts 37:1–23

Weston NB, Dixon RE, Joye SB (2006) Ramifications of increased salinity in tidal freshwater sediments: geochemistry and microbial pathways of organic matter mineralization. J Geophys Res Biogeosci 111:G01009. doi:10.1029/2005JG000071

Weston NB, Vile MA, Neubauer SC, Velinsky DJ (2011) Accelerated microbial organic matter mineralization following salt-water intrusion into tidal freshwater marsh soils. Biogeochemistry 102(1–3):135–151

Westrich JT, Berner RA (1988) The effect of temperature on rates of sulfate reduction in marine sediments. Geomicrobiol J 6:99–117

Whigham DF (1978) Relationship between aboveground and belowground biomass of freshwater tidal wetland macrophytes. Aquat Bot 5(4):355–364

Whigham D, Simpson R (1977) Growth, mortality, and biomass partitioning in freshwater tidal wetland populations of wild rice (*Zizania-aquatica*-var-*aquatica*). Bull Torrey Bot Club 104(4):347–351

Whigham DF, McCormick J, Good RE, Simpson RL (1978) Biomass and primary production in freshwater tidal wetlands of the middle Atlantic Coast. In: Good RE, Whigham DF, Simpson RL (eds) Freshwater wetlands: ecological processes and management potential. Academic Press, New York, pp 3–20

Whiting GJ, Chanton JP (1993) Primary production control of methane emission from wetlands. Nature 364(6440):794–795

Whiting GJ, Chanton JP (1996) Control of the diurnal pattern of methane emission from emergent aquatic macrophytes by gas transport mechanisms. Aquat Bot 54:237–253

Whiting GJ, Chanton JP (2001) Greenhouse carbon balance of wetlands: methane emission versus carbon sequestration. Tellus Ser B Chem Phys Meteorol 53(5):521–528

Whiting GJ, Bartlett DS, Fan SM, Bakwin PS, Wofsy SC (1992) Biosphere atmosphere CO_2 exchange in tundra ecosystems: community characteristics and relationships with multispectral surface reflectance. J Geophys Res Atmos 97(D15):16671–16680

Willis JM, Hester MW (2004) Interactive effects of salinity, flooding, and soil type on *Panicum hemitomon*. Wetlands 24(1):43–50